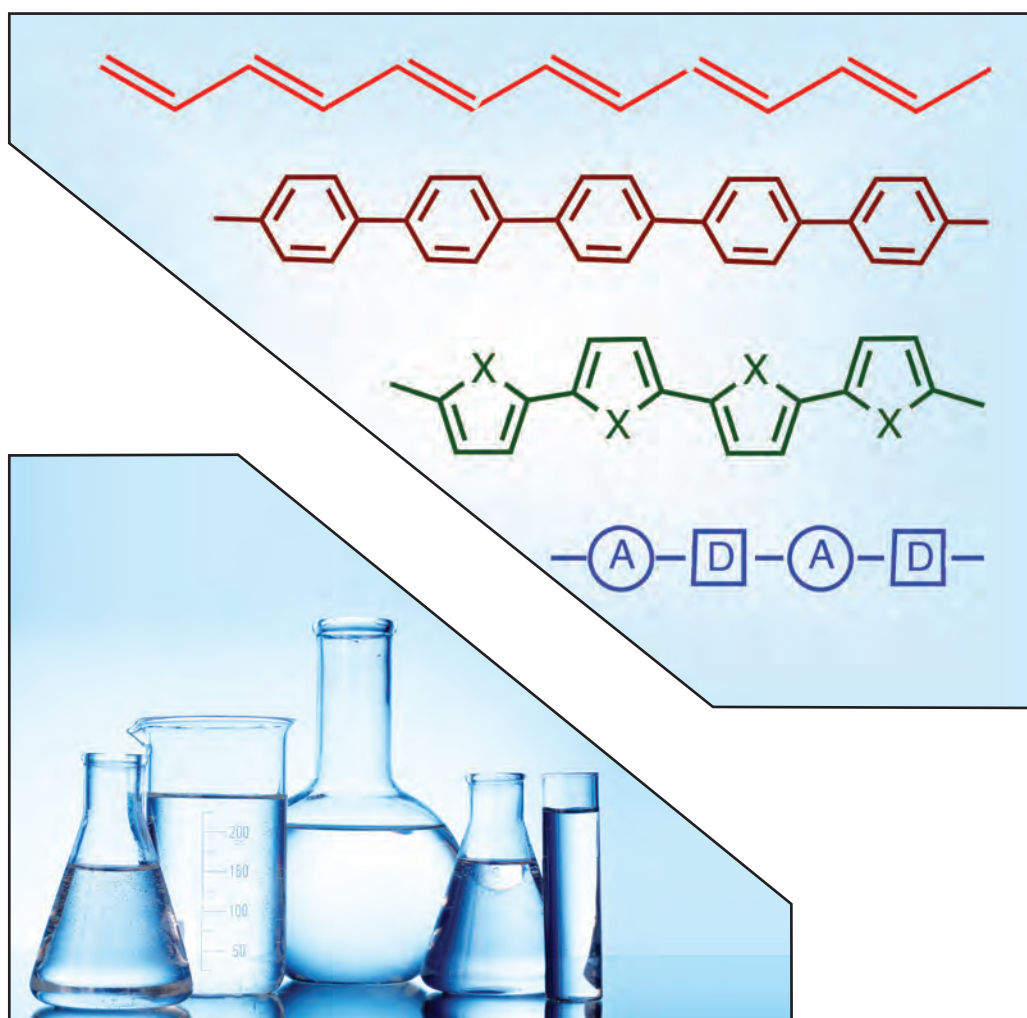


RSC Polymer Chemistry Series

Edited by Klaus Müllen, John R Reynolds and Toshio Masuda

Conjugated Polymers

A Practical Guide to Synthesis



RSC Publishing

Conjugated Polymers

A Practical Guide to Synthesis

RSC Polymer Chemistry Series

Series Editors:

Professor Ben Zhong Tang (Editor-in-Chief), *The Hong Kong University of Science and Technology, Hong Kong, China*

Professor Alaa S. Abd-El-Aziz, *University of Prince Edward Island, Canada*

Professor Stephen L. Craig, *Duke University, USA*

Professor Jianhua Dong, *National Natural Science Foundation of China, China*

Professor Toshio Masuda, *Fukui University of Technology, Japan*

Professor Christoph Weder, *University of Fribourg, Switzerland*

Titles in the Series:

- 1: Renewable Resources for Functional Polymers and Biomaterials
- 2: Molecular Design and Applications of Photofunctional Polymers and Materials
- 3: Functional Polymers for Nanomedicine
- 4: Fundamentals of Controlled/Living Radical Polymerization
- 5: Healable Polymer Systems
- 6: Thiol-X Chemistries in Polymer and Materials Science
- 7: Natural Rubber Materials: Volume 1: Blends and IPNs
- 8: Natural Rubber Materials: Volume 2: Composites and Nanocomposites
- 9: Conjugated Polymers: A Practical Guide to Synthesis

How to obtain future titles on publication:

A standing order plan is available for this series. A standing order will bring delivery of each new volume immediately on publication.

For further information please contact:

Book Sales Department, Royal Society of Chemistry, Thomas Graham House, Science Park, Milton Road, Cambridge, CB4 0WF, UK

Telephone: +44 (0)1223 420066, Fax: +44 (0)1223 420247

Email: booksales@rsc.org

Visit our website at www.rsc.org/books

Conjugated Polymers

A Practical Guide to Synthesis

Edited by

Klaus Müllen

Max Planck Institute for Polymer Research, Germany

Email: muellen@mpip-mainz.mpg.de

John R. Reynolds

Georgia Institute of Technology, USA

Email: reynolds@chemistry.gatech.edu

and

Toshio Masuda

Fukui University of Technology, Japan

Email: masuda@fukui-ut.ac.jp

RSC Publishing

RSC Polymer Chemistry Series No. 9

ISBN: 978-1-84973-799-9

ISSN: 2044-0790

A catalogue record for this book is available from the British Library

© The Royal Society of Chemistry 2014

All rights reserved

Apart from fair dealing for the purposes of research for non-commercial purposes or for private study, criticism or review, as permitted under the Copyright, Designs and Patents Act 1988 and the Copyright and Related Rights Regulations 2003, this publication may not be reproduced, stored or transmitted, in any form or by any means, without the prior permission in writing of The Royal Society of Chemistry, or in the case of reproduction in accordance with the terms of licences issued by the Copyright Licensing Agency in the UK, or in accordance with the terms of the licences issued by the appropriate Reproduction Rights Organization outside the UK. Enquiries concerning reproduction outside the terms stated here should be sent to The Royal Society of Chemistry at the address printed on this page.

The RSC is not responsible for individual opinions expressed in this work.

Published by The Royal Society of Chemistry,
Thomas Graham House, Science Park, Milton Road,
Cambridge CB4 0WF, UK

Registered Charity Number 207890

For further information see our web site at www.rsc.org

*This book is dedicated to our spouses, Renate Müllen,
Dianne Reynolds and Keiko Masuda, for the understanding and support
they have given us in all that we do.*

Preface

Why conjugated polymers? A convincing answer to this question can be given in three parts: conjugated polymers are fascinating species from i) a structural point of view due to the many ways of establishing an extended pi-conjugation; ii) a functional point of view due to their electronic and optical properties, which qualify them as active components of organic electronics; and iii) a research point of view due to their potential of fostering cross-disciplinary research.

Since we live in a material world there cannot be novel technology without new or improved materials, and they must be synthesized. Synthesis is both a matter of creative design and experimental skill, and no target structure can prove this claim better than conjugated polymers. The crucial role of synthesis is what has led to the concept of this book; not so much as a theoretical exercise “on-paper”, but as a practical, “hands-on” approach. It is intended to convince the reader of the beauty of conjugated polymer design and synthesis, but not set aside the technical difficulties and experimental pitfalls.

A good case can be made by first taking a look at the device and then work backwards to the synthesis of the functional molecules. Technologies and also the underlying materials stand in competition with each other. Organic electronics face the fact that inorganic semiconductors, such as silicon, have beautiful properties and are thus strong contenders. One may think of the high charge carrier mobilities and the vanishing exciton binding energy. What stands against that is the “designable” structural and functional versatility of their organic counterparts, highlighted by the ease of their synthesis and processing. Even in the organic field, conjugated polymers must compete with small organic molecules, which can be made structurally perfect and can be processed by vacuum techniques.

Whatever material is considered, organic synthesis is generally performed in solution. The active function of an organic electronic device, however, cannot

be understood or even tailored by restricting one's attention to the dilute solution. It is rather a matter of solid thin films and their interfaces. An important criterion, when judging the function of an organic field effect transistor (OFET) as a switch, is high charge carrier mobility. This depends upon the solid state packing and thus the supramolecular order of the semiconductor. Likewise, "bright" emission from an organic light emitting diode (OLED) requires different layers with defined interfaces to keep the charge recombination zone away from the metal electrode; and this, next to high film quality, depends upon the orthogonal solubility of the different conjugated polymers used. The situation in an organic photovoltaic device (OPV) is, from a morphological point of view, even more complex. What is needed in such a device is a nanophase separation of electron donor and electron acceptor components to ensure, after charge separation, efficient percolation of holes and electrons. It is the complexity of the underlying functional processes that explains why physics, engineering and materials science are so important – or at least have the last say when it comes to device performance and stability.

Again, the whole endeavor starts with synthesis and this shall be considered in greater detail now. Even the more distant reader will be aware of "classical" conjugated polymer structures, such as poly(*p*-phenylene) (PPP), poly(phenylenevinylene) (PPV) and polythiophene (PT). Here the "usual suspects" are incorporated as building blocks: benzene, thiophene or a C=C double bond. It does not need much imagination, however, to dream up structural modifications, which brings us to the unbelievable manifold of design opportunities. When we take a closer look at the nature of the building blocks, benzene can be replaced by larger polycyclic aromatic hydrocarbons (PAHs) that also leave us with different ring positions as coupling points. Hydrocarbons can be replaced by their heterocyclic analogues, which is particularly important for the electron donor or acceptor character of the final macromolecule. The search for even more repeat units can have different driving forces, empirical or theoretical, and is often coupled to device results. This can also explain why the community sometimes follows fashion. Presently, donor units, such as bridged dithiophenes, and acceptor units, such as benzothiadiazole or diketopyrrolopyrrole, seem to be particularly popular. When different building blocks are incorporated there are many ways of doing this, statistically or in a defined sequence. Conjugated polymers with an alternating array of donor and acceptor repeat units have been studied as low band gap materials for efficient light harvesting in OPV. Another important structural modification becomes possible by an increase in the dimensionality of the macromolecules when going from a (linear) chain to a step ladder or even full ladder polymer. A logical extension then is a true two-dimensional pi-system, such as a graphene sheet, which has recently attracted immense attention. Finally, all these polymer architectures possess inherent rigidity that can severely limit solubility and thus solution processability. Alkyl substitution is therefore a mandatory step. There is of course, the danger of compromising extended conjugation when the additional substituent causes torsion of the building blocks about the interring bonds, and substituents may be considered

to “dilute” electronic properties. Nevertheless, alkyl substituents can also have beneficial effects by directing supramolecular order during film formation. This is also true when more complex topologies are targeted, such as diblock or multiblock copolymers made from rod or coil segments. The latter aspect is not only relevant for electronic reasons – bringing electron rich and electron poor domains into close proximity to one another – but also for morphological reasons, where phase separation can be enforced at the desired length scale.

All these design opportunities concern the macromolecular structure – prior to processing – and they are, indeed, decisive for key electronic and optical features, such as, for example, the wavelength of absorption and emission or their function as n-type *vs.* p-type semiconductors. One might go as far as to claim that, based on these subtle structure–property relationships, (opto)electronic properties can be “synthesized”. Or one might even go a step further and encode desired supramolecular characteristics to introduce weak intermolecular forces during molecular design, although in this case structure–property relationships are much less well developed. Here is, however, a very critical point: all these design opportunities are easily sketched on paper but do not necessarily translate easily into a glass flask. This brings us to the key issue of this book: the synthesis of conjugated polymers.

When talking about conjugated polymer synthesis, an initial question concerns the availability and purity of the suitably functionalized building blocks. Thereby, the required synthetic efforts can be quite different and demands by the community can lead to the commercial availability of starting compounds. Closely connected to this is the question of the polymerization reaction, that is to say how the building blocks are subjected to a repetitive coupling. Remarkably enough, while step-growth methods have long been the “classical” polymerization mode, chain-growth methods have recently been realized as well. This of course holds promise for establishing “living” end-groups and offers new opportunities for block copolymer synthesis. Transition metal-catalyzed reactions developed in organic and organometallic chemistry have had a huge impact on conjugated polymer synthesis, and this holds true for methods not only of carbon-carbon, but also carbon-heteroatom (*e.g.* nitrogen) connections. Many of these commonly used pathways are addressed as “named reactions” honoring their inventors and, indeed, these inventions can hardly be overestimated. These reactions allow the connection of aromatic ring systems to a polymer chain *via* homo- or hetero-atom couplings, and there the reader will readily envisage how important the above mentioned strictly alternating incorporation of donor and acceptor moieties is. Apart from aromatic building blocks, vinylene and ethynylene elements can be introduced as well. Here it is rewarding to compare transition-metal catalysis with older procedures, such as connective double-bond formation.

Is it thus sufficient, when targeting a particular polymer structure, to check the literature for the right building blocks and the best mode of coupling? The answer is definitely no, and there are at least two reasons for that. The first one, even if somewhat discouraging for a physicist who feels that the synthetic plan looks quite easy, concerns the experimental conditions. A typical case is

rigorous exclusion of oxygen and water since these can affect catalyst activity and trigger unwanted side-reactions. The choice of reaction temperature and time should be mentioned here as well. The second reason is that the nature of the building block and the chosen synthetic method must be carefully adjusted. Thus, steric hindrance may slow down the growth of the macromolecule so much that side reactions come into play, which can either stop further growth or induce side reactions. The issue of side reactions, even if occurring as minor processes, is critical. A typical case is the so-called Wessling Zimmermann synthesis of PPV, which played an important role for the development of light emitting devices based upon conjugated polymers in the early nineties. This advance in the synthetic procedure was achieved *via* a precursor polymer, which was finally transformed into the conjugated chain *via* a 1,2-elimination process. Failure to accomplish this quantitatively will, of course, lead to an interrupted pi-conjugation. Even more severe is the fact that side reactions can lead to (ketonic) defects that act as traps for the excited states of the light emitting device. Let us come back to the question of the mechanism of the polymer forming reaction. In a step-growth polycondensation, high molecular weights can only be achieved for high degrees of conversion and thus the coupling of intermediate oligomers. Even if limitations imposed by solubility can be excluded, mismatch of the stoichiometries must be avoided, and this relates to the absence of side reactions.

Conjugated polymer synthesis, in order to be meaningful, requires an even higher level of sophistication, and this raises the question of how we describe its molecular structure. We commonly denote the prevailing repeat units, written in parenthesis, and then add “*n*” for the number of repeat units, even if it is often not specified. There are ample cases, particularly in recent literature, where the molecular weight and the polydispersity of an individual polymer play a decisive role in the device performance, such as charge carrier mobility. This, by the way, can readily be understood when considering the above mentioned ordered packing of polymer chains. Then, it is clear that further features come into play, such as the mode of end-capping. Impurities, as has been mentioned, can serve as traps not only for excitons, but also for charges, and structural irregularities do not only interrupt pi-conjugation, but also hamper regular packing. It follows that the above way of denoting a polymer is in urgent need of careful specification. Otherwise, the whole research field is in danger of criticism, such as “*they measure very precisely, but they do not precisely know what they measure*”.

This book is intended to show the beauty of conjugated polymer synthesis without ignoring the difficulties and obstacles. While organic electronics are often tempted to follow the fascination of device fabrication, this book takes the opposite direction in a synthesis-first approach. This approach requires imagination, but also scrupulous optimization of experimental conditions combined with careful proof of structural perfection.

Considering the above, a strong plea is made herein to activate the good old virtues of organic synthesis, and these will certainly prove their value when, for example, pushing the limits of molecular weight or handling a low band gap

polymer with its inherent chemical instability. There are, however, still many open territories for conjugated polymer synthesis. The new challenges could concern a complex combination of properties, such as making a charge transporting polymer also responsive to stimulus-driven switching or by connecting a conjugated polymer segment to a biomacromolecule for recognition and self-assembly processes. Furthermore, while we have so far focused on the power of solution synthesis, performing synthesis in the (bulk) solid state or on a surface could create significant advantages as one could not only build in the supramolecular order, but also avoid the additional difficulties of controlling solution processing. Whether synthesis is structure or method oriented, knowledge or application driven, or whether it targets new polymer structures or up-scales established ones, it finds room everywhere. But it is not always easy. However, we believe that this book will help to make it easier – and more successful.

Last but not least, we would like to thank all the authors who actively do research in the forefront of the conjugated polymer field for their excellent contributions. Thanks are also due to Professor Ben Zhong Tang, Editor-in-Chief of this book series for his continuous support and to Ms. Leanne Marle at the RSC office for her clerical assistance.

Klaus Müllen
On behalf of the Editors

Contents

Chapter 1	Pi-Conjugated Polymers: The Importance of Polymer Synthesis	1
	<i>John R. Reynolds</i>	
1.1	Historical Perspective	1
1.2	Considerations in Polymerizations	3
1.3	Side Chains, Processability and Molecular Weight	4
1.4	Structural Control <i>via</i> Repeat Unit and Functionality	5
1.5	Summary	9
	Acknowledgements	10
	References	10
Chapter 2	Polyacetylenes	12
	<i>Kazuo Akagi</i>	
2.1	Introduction	12
2.1.1	Polyacetylene (PA)	13
2.1.2	Helical Polyacetylene (H-PA)	18
2.1.3	H-PA with Bundle-Free Fibril Morphology	24
2.1.4	Morphology-Retaining Carbonization of H-PA	28
2.2	Experimental Procedures	29
2.2.1	Synthesis of Shirakawa-Type PA	29
2.2.2	Synthesis of Naarmann and Theophilou-Type PA	29
2.2.3	Synthesis of Tsukamoto-Type PA	30
2.2.4	Synthesis of High Mechanical Modulus and Strength PA	30
2.2.5	Synthesis of Directly Aligned PA	31

RSC Polymer Chemistry Series No. 9

Conjugated Polymers: A Practical Guide to Synthesis

Edited by Klaus Müllen, John R. Reynolds and Toshio Masuda

© The Royal Society of Chemistry 2014

Published by the Royal Society of Chemistry, www.rsc.org

2.2.6	Synthesis of Helical PA	32
2.2.7	Synthesis of Nematic Liquid Crystals and Chiral Dopants	32
	References	33
Chapter 3	Substituted Polyacetylenes	37
	<i>Fumio Sanda, Masashi Shiotsuki and Toshio Masuda</i>	
3.1	Introduction	37
3.1.1	Polymers of Aromatic Monosubstituted Acetylenes	38
3.1.2	Polymers of Aliphatic Monosubstituted Acetylenes	39
3.1.3	Polymers of Aromatic Disubstituted Acetylenes	39
3.1.4	Polymers of Aliphatic Disubstituted Acetylenes	40
3.1.5	Functions of Substituted Polyacetylenes	41
3.2	Experimental Procedures	42
3.2.1	Materials and General Polymerization Procedures	42
3.2.2	Polymers of Aromatic Monosubstituted Acetylenes	43
3.2.3	Polymers of Aliphatic Monosubstituted Acetylenes	49
3.2.4	Polymers of Aromatic Disubstituted Acetylenes	51
3.2.5	Polymers of Aliphatic Disubstituted Acetylenes	54
3.2.6	Characterization and Remarks	56
	References	58
Chapter 4	Polyphenylenes	61
	<i>Takakazu Yamamoto</i>	
4.1	Introduction	61
4.1.1	Polyphenylenes without Side Chain	62
4.1.2	Polyphenylenes with Side Chains or Side Rings	65
4.2	Experimental Procedures	66
4.2.1	Materials and General Polymerization Procedures	66
4.2.2	Polyphenylenes without Side Chain	67
4.2.3	Polyphenylenes with Side Chains	71
4.2.4	Polyphenylenes with -N=N- or -NR- Binding Units	77
4.2.5	Polyphenylenes with Conjugated Side Rings	79

4.2.6	Polyphenylenes with -SO ₃ M or -NO ₂ Side Chains Prepared <i>via</i> Ullmann Coupling	80
4.2.7	Characterization and Remarks	81
	References	82
Chapter 5	Polyfluorenes	87
	<i>Byung Jun Jung, Hong-Ku Shim and Do-Hoon Hwang</i>	
5.1	Introduction	87
5.2	Experimental Procedures	88
5.2.1	Oxidative Polymerization	88
5.2.2	Yamamoto Coupling Polymerization	89
5.2.3	Suzuki Coupling Polymerization	92
5.3	Developments in Polymerization	99
5.3.1	Microwave-Assisted Polymerization	99
5.3.2	Other Synthetic Techniques	99
5.3.3	New Polymerization Methods	99
5.3.4	Purification of Polymers	100
5.4	Various Applications of Polyfluorenes	101
5.4.1	Polymer Light-Emitting Diodes (PLEDs)	101
5.4.2	Sensing Applications	105
5.4.3	Polymer Transistors and Solar Cells	105
5.4.4	Electron Injection Layers in Organic Electronic Devices	107
5.5	Remarks	107
	References	108
Chapter 6	Poly(carbazolylene)s	113
	<i>Sung Ju Cho and Andrew C. Grimsdale</i>	
6.1	Introduction	113
6.1.1	Poly(3,6-carbazolylene)s	114
6.1.2	Poly(1,8-carbazolylene)s	116
6.1.3	Poly(2,7-carbazolylene)s	116
6.1.4	Poly(3,9-carbazolylene)s	119
6.1.5	Ladder-Type Polycarbazolylenes	120
6.2	Experimental Procedures	121
6.2.1	Materials and General Procedures	121
6.2.2	Poly(3,6-carbazolylene)s	121
6.2.3	Poly(1,8-carbazolylene)s	123
6.2.4	Poly(2,7-carbazolylene)s	124
6.2.5	Poly(3,9-carbazolylene)s	128
6.2.6	Ladder-Type Poly(carbazolylene)s	129
	References	132

Chapter 7	Poly(phenylenevinylene)s	134
	<i>Wallace W. H. Wong, Helga Seyler and Andrew B. Holmes</i>	
7.1	Introduction	134
7.2	Methods of Synthesis	135
7.2.1	Precursor Routes <i>via</i> Radical/Anionic Polymerization Mechanism	135
7.2.2	Direct Routes to PPVs: Step-growth Polycondensation	140
7.2.3	Ring-Opening Metathesis Polymerization	144
7.2.4	Alternative Routes	145
7.2.5	Comparison of Syntheses and Summary	146
7.3	Experimental Procedures	147
7.3.1	General Experimental Requirements	147
7.3.2	Example Procedures	148
	References	151
Chapter 8	Poly(p-phenyleneethynylene)s and Poly(aryleneethynylene)s	156
	<i>Uwe H. F. Bunz</i>	
8.1	Introduction	156
8.1.1	Alkyl-PPEs and PAEs by Alkyne Metathesis	159
8.1.2	Alkyl-PPEs by Pd Catalysis	161
8.1.3	Alkoxy-PPEs by Pd Catalysis	162
8.1.4	Poly(flourenyleneethynylene)s by Alkyne Metathesis	163
8.1.5	Other PAEs by Pd Catalysis	164
8.1.6	Side-Chain Functionalized PPEs by Pd-Catalyzed Coupling	165
8.2	Experimental Procedures	165
8.2.1	Materials and General Polymerization Procedures	165
8.2.2	Didodecyl-PPE 13b by Alkyne Metathesis of 12b	168
8.2.3	Sonogashira Reactions, General Remarks	168
8.2.4	Polyfluorenyleneethynylene by ADIMET	171
8.2.5	Quinoxaline-Containing PAEs	171
8.2.6	Benzothiadiazole-Containing PAE	173
8.2.7	Quinoline-Containing PAEs	173
8.2.8	Grafted PPEs	174
8.2.9	Characterization and Concluding Remarks	176
	References	177

<i>Contents</i>	xvii
Chapter 9 Polythiophenes	180
<i>Dahlia Haynes and Richard McCullough</i>	
9.1 Introduction	180
9.1.1 Synthesis of Nonsubstituted Polythiophenes (PT)s	181
9.1.2 Synthesis of Regioirregular Substituted Polythiophenes (PST)	182
9.1.3 Synthesis of Regioregular Poly(Substituted Thiophenes) (<i>rr</i> -P3STs)	184
9.2 Experimental Procedures	187
9.2.1 Nonsubstituted Polythiophenes	187
9.2.2 Syntheses of Regioirregular Substituted Polythiophenes	189
9.2.3 Syntheses of Regioregular Substituted Polythiophenes	191
9.2.4 General Procedures and Characterization	196
9.3 Conclusion and Outlook	196
References	197
Chapter 10 Poly(oxythiophene)s	201
<i>Anil Kumar, Sreelekha P. Gopinathan and Rekha Singh</i>	
10.1 Introduction	201
10.1.1 Polymerization Processes	202
10.1.2 Poly(3-oxythiophene)s	202
10.1.3 Poly(3,4-dioxythiophene)s	203
10.1.4 Miscellaneous Poly(oxythiophene)s	204
10.2 Experimental Procedures	204
10.2.1 Oxidative Polymerization	208
10.2.2 Transition-Metal-Assisted Polymerization	215
10.3 Concluding Remarks	218
References	219
Chapter 11 Polypyrroles	224
<i>Pierre Audebert and Fabien Miomandre</i>	
11.1 Introduction	224
11.2 Polypyrrole Electrosynthesis	225
11.2.1 Overview	225
11.2.2 Experimental Procedures	228
11.3 Polypyrroles – Chemical Syntheses	234
11.3.1 Overview	234
11.3.2 Classical Polypyrrole Synthesis through Pyrrole Oxidation	235
11.3.3 Experimental Procedures	238
References	244

Chapter 12 Polyanilines	248
<i>Jacob Tarver and Yueh-Lin Loo</i>	
12.1 Introduction	248
12.1.1 Synthesis Mechanism	250
12.2 Experimental Procedures	250
12.2.1 Chemical Polymerization of Anilines	251
12.2.2 Electrochemical Polymerization of Anilines	256
12.2.3 Template Polymerization of Anilines	257
12.2.4 Secondary Doping of Polyanilines	260
12.2.5 Characterization and Remarks	261
References	262
Chapter 13 Si–Si Bond Polymers, Oligomers, Molecules, Surface, and Materials	265
<i>Michiya Fujiki</i>	
13.1 Hierarchy of the Si–Si Bond Family: From Gaseous SiH ₄ to Crystal Silicon	265
13.2 Polymerization Techniques	266
13.2.1 Wurtz-Type Condensation – The Most Versatile Method	266
13.2.2 Electrochemical Reduction	267
13.2.3 Ring-Opening Reactions with Precursors	267
13.2.4 Dehydrogenative Coupling with Organometallic Catalysts	268
13.2.5 Postpolymerization toward Functionalization	268
13.2.6 Chemical Modification of Si–H Bonds at the Surface of Crystal Silicon	268
13.2.7 Deintercalation from the Zintl Phase – An Ideal Two-Dimensional Si Skeleton	268
13.2.8 Thermolysis	269
13.3 Features of Si–Si Bond Family Members	270
13.3.1 Chain-Like Polysilanes and Oligosilanes	270
13.3.2 Cyclic Four-Membered Oligosilanes and Ladder Oligosilanes	278
13.3.3 Network-Like Organopolysilanes (Organopolysilylene)	278
13.3.4 Chemical Modification of Ideal Two-Dimensional Si–Si Polymers with CaSi ₂	279
13.3.5 Highly Strained Persila-Polyhedra	279
13.3.6 Exotic Unsaturated Multiple Si–Si Bond Compounds	281
13.3.7 Surface Modification of Si–C Linkages from <i>c</i> -Si with Si–H Bond	283

<i>Contents</i>	xix
13.4 Experimental Procedures	285
13.4.1 Poly(diarylsilane)s	285
13.4.2 Fluoroalkylpolysilane Homo- and Copolymers	287
13.4.3 Poly(alkylarylsilane) Homo- and Copolymers	288
13.4.4 Poly(alkylsilyne)s and Vacuum Pyrolysis	290
References	291
Chapter 14 Alternating Polyheterocycles	296
<i>Kazuo Tanaka and Yoshiki Chujo</i>	
14.1 Introduction	296
14.1.1 Alternating Polymers of Boron	297
14.1.2 Alternating Polymers of Silicon	301
14.1.3 Alternating Polymers of Germanium	303
14.1.4 Alternating Polymers of Phosphorus	304
14.1.5 Alternating Polymers of Transition Metals	305
14.2 Experimental Procedures	305
14.2.1 Materials and General Polymerization Procedures	305
14.2.2 Alternating Polymers of Boron	307
14.2.3 Alternating Polymers of Silicon	311
14.2.4 Alternating Polymers of Germanium	312
14.2.5 Alternating Polymers of Phosphorus	313
14.2.6 Alternating Polymers of Transition Metals	314
References	316
Chapter 15 Donor–Acceptor Alternating Copolymers	319
<i>Wentao Li and Wei You</i>	
15.1 Introduction	319
15.1.1 Inception of the Concept of D–A Alternating Copolymers	320
15.1.2 Advantages of D–A Alternating Copolymers and the State-of-the-Art	320
15.2 General Methods for D–A Copolymerization	322
15.2.1 Suzuki Reaction vs. Stille Reaction	322
15.2.2 Factors to Consider from the Perspective of Stille Polymerization	323
15.2.3 Factors to Consider from the Perspective of Suzuki Polymerization	324
15.2.4 Factors to Consider from the Perspective of Step Growth	325
15.2.5 New Development: Direct Arylation and Chain-Growth Polymerization	327

15.3	Synthesis of Selected Monomers and Typical Polymerizations	328
15.3.1	Synthesis of Donor Monomers	328
15.3.2	Synthesis of Acceptor Monomers	330
15.3.3	Purification of Reagents	334
15.3.4	Typical Procedure of Polymerization and Purification of Product	335
15.3.5	Representative Syntheses of D–A Alternating Copolymers	336
15.3.6	Characterization and Remarks	338
	References	338
Chapter 16	Conjugated Polyelectrolytes	343
	<i>Anand Parthasarathy, Xuzhi Zhu and Kirk S. Schanze</i>	
16.1	Introduction	343
16.1.1	A Brief History of Conjugated Polyelectrolytes	344
16.1.2	Synthesis of Conjugated Polyelectrolytes – General Considerations	345
16.1.3	Conjugated Polyelectrolyte Synthesis by the Direct Approach	346
16.1.4	Conjugated Polyelectrolyte Synthesis by the Precursor Method	348
16.2	Experimental Procedures	350
16.2.1	Materials and General Considerations	350
16.2.2	Example Procedures	351
	References	357
Chapter 17	Self-Doped Polymers	359
	<i>M. Ramesh Kumar and Michael S. Freund</i>	
17.1	Introduction	359
17.1.1	Self-Doped Conducting Polymers	359
17.1.2	Types and Classes	361
17.1.3	Doping Mechanisms and Properties	362
17.2	Experimental Procedures	363
17.2.1	Common Synthetic Mechanisms and Outcomes	363
17.2.2	Common Methods of Characterization	366
17.2.3	Polyanilines	369
17.2.4	Polypyrroles	375
17.2.5	Polythiophenes	376
17.2.6	Polycarbazoles	379
17.2.7	Poly(<i>p</i> -phenylene)s	379
17.2.8	Poly(phenylenevinylene)s	380

<i>Contents</i>	xxi
17.2.9 Polyindoles	381
17.2.10 Polyacetylenes	382
References	383
Chapter 18 Fused Heterocycle Polymers	387
<i>Sandeep Kaur, Alexander L. Kanibolotsky and Peter J. Skabara</i>	
18.1 Introduction	387
18.1.1 Dithiin-Based Polymers	389
18.1.2 Tetrathiafulvalene (TTF)-Based Polymers	391
18.1.3 Diketopyrrolopyrrole (DPP)-and Thieno[3,4- <i>c</i>]pyrrole-4,6-dione (TDP)-Based Polymers	392
18.1.4 4,4-Difluoro-4-boro-3a-4a-diaza- <i>s</i> -indacene (BODIPY)- and Isoindigo (iI)-Based Polymers	395
18.1.5 Azole- and Pyrazine-Based Polymers	397
18.2 Experimental Procedures	400
18.2.1 Materials and General Polymerization Procedures	400
18.2.2 Dithiin-Based Polymers	401
18.2.3 TTF-Based Polymers	403
18.2.4 DPP- and TDP-Based Polymers	406
18.2.5 BODIPY- and Isoindigo-Based Polymers	410
18.2.6 Azole- and Pyrazine-Based Polymers	412
18.2.7 Characterization and Remarks	418
References	419
Chapter 19 Direct Arylation/Heteroarylation Polycondensation Reactions	422
<i>Lauren G. Mercier, Agnieszka Pron and Mario Leclerc</i>	
19.1 Introduction	422
19.2 Reaction Conditions	423
19.2.1 General Comments	423
19.2.2 Heck (Jeffery) Conditions	424
19.2.3 Carboxylic Acid Additives	425
19.2.4 Without Carboxylic Acid Additives	427
19.3 Mechanistic Investigations	430
19.4 Experimental Procedures	433
19.4.1 Materials and General Polymerization Procedures	433
19.4.2 Polymerization Using Heck (Jeffery) Conditions	434

19.4.3	Polymerization with Carboxylic Acid Additives	434
19.4.4	Polymerization without Carboxylic Acid Additives	437
19.5	Conclusions	439
	References	440
Chapter 20	Chain-Growth Catalyst-Transfer Polycondensations	443
	<i>Anton Kiriya and Volodymyr Senkovskyy</i>	
20.1	Catalyst-Transfer Polycondensation: Mechanism, Scope and Limitations	443
20.1.1	Introduction	443
20.1.2	Mechanism	444
20.1.3	End-Functionalized Polymers and Brushes	446
20.1.4	Fully Conjugated Block Copolymers	447
20.1.5	Chain-Growth Polymerization of Electron-Deficient Monomers	449
20.1.6	Chain-Growth Suzuki Polycondensation	449
20.1.7	Perspective	451
20.2	Experimental Procedures	452
20.2.1	Polythiophenes	452
20.2.2	Polyfluorenes, Polycarbazoles, Polyphenylenes and Alternating Copolymers	453
20.2.3	End-Functionalized Polymers, Stars and Brushes	455
20.2.4	Rod-Coil Block Copolymers	459
20.2.5	All-Conjugated Block Copolymers	461
20.2.6	Suzuki Polymerization	465
	References	467
	Subject Index	471

CHAPTER 1

Pi-Conjugated Polymers: The Importance of Polymer Synthesis

JOHN R. REYNOLDS

School of Chemistry and Biochemistry, School of Materials Science and Engineering, Center for Organic Photonics and Electronics, Georgia Institute of Technology, 901 Atlantic Drive, Atlanta, GA 30332-0400, USA
Email: reynolds@chemistry.gatech.edu

1.1 Historical Perspective

When one considers the early days of conjugated and conducting polymer synthesis, the early work by Letheby on the oxidation of aniline, presumably forming polyaniline (**1**),¹ and Dall'Olio *et al.* on polypyrrole (**2**)² are often referred to as landmark developments in the field. To gain an important historical view, the reader is directed to the work of Rasmussen who provides a perspective on the field where the work of Weiss on polypyrrole, as well as that of Buvet and Jozefowicz on polyaniline, are highlighted.³ These materials, while completely insoluble and infusible as formed from oxidative polymerization from the parent monomers, served as the basis for inducing electroactivity into polymer systems. Over the years, numerous review articles, book chapters and reviews have issued around the field, most often directed to a class of polymers or type of property they impart, with the 1986, 1998, and 2007 editions of the “Handbook of Conducting Polymers” providing a deep and complete scientific overview⁴⁻⁶ (Chart 1.1).

The 1950s saw the Nobel Prize winning work of Karl Ziegler and Giulio Natta on coordination polymerization of unsaturated molecules, which

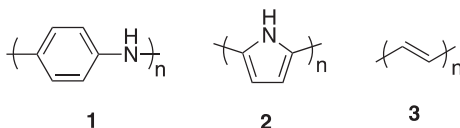


Chart 1.1

provided a route to structurally well-defined polymers.⁷ Most known for the development of commercially important polyolefins (*e.g.* polyethylene and polypropylene), the work of Natta demonstrated that acetylene polymerization could yield the conjugated polymer polyacetylene $(\text{CH})_x$ (**3**) as an infusible grey powder.⁸ While the 1960s saw the development of many aromatic units containing polymers, it also became understood that pi-conjugation led to semi-conducting material properties. In one fascinating study, Berets and Smith⁹ examined the vapor phase treatment of $(\text{CH})_x$ powders with various Lewis acids and bases. In fact, when using BF_3 as the reacting dopant, they measured conductivity enhancements by a factor of 1000 on pressed pellets. In this work, they also treated $(\text{CH})_x$ with Cl_2 , yet only saw small conductivity increases by a factor of 5. Interestingly for the discussion that will follow, this work did not use iodine or bromine as an oxidizing system.

Serendipity and careful observation go hand-in-hand in science, and this has been especially important for many discoveries in the conjugated and conducting polymer field. An especially important discovery was the formation of free-standing films of $(\text{CH})_x$ by Ito *et al.* in 1974 caused by rapid polymerization of acetylene at a quiescent Ziegler–Natta polymerization initiator system solution.¹⁰ While the Shirakawa research group was mainly dedicated to understanding structural properties (*e.g.* *cis–trans* ratios), the fact that these films were mechanically flexible, with a metallic silver luster, suggested important underlying electronic properties.

In a landmark series of experiments, Heeger, MacDiarmid, and Shirakawa combined efforts to study the electronic properties and gas-phase doping of polyacetylene films. Their discovery that treatment of these films with controlled amounts of Cl_2 , Br_2 , I_2 and AsF_5 could yield conductivity enhancements greater than 10^7 , and ultimately yield electronic conductivities in excess of 500 S/cm, demonstrated unprecedented conductivity in an organic polymer.¹¹ While charge transfer salts, such as those based on tetrathiafulvalene and tetracyanoquinodimethane were known to exhibit high conductivity and metallic properties,¹² the fact that such properties were accessible in the more disordered and flexible polymer films was especially stunning. Researchers around the world quickly picked up on this, and it was demonstrated that the high level of conjugation in the polymer, along with pi-stacking and interchain interactions, all played an important role in the electronic properties. Chemists quickly realized that many polymer structures could be prepared that were fully conjugated; thus, the stage was set for a major synthetic effort. This work has now spanned 30 years and has led from insoluble, infusible, materials that were highly unstable conductors to

well-characterized, solution processable polymers with fine structural control that are finding utility across a broad number of applications.

With this background in mind, this book seeks to teach the details of synthetic preparative polymer chemistry in all of the major classes of pi-conjugated polymers that have been developed to researchers in the field. The authors of each chapter have carefully overviewed the various polymer types employed in the field with a special focus on experimental details that yield reproducible and high-quality materials. Prior to moving to those specific chapters, let's take some time to review the general concepts in polymerization that are important for the development of such materials.

1.2 Considerations in Polymerizations

Fundamental polymer chemistry teaches us two main relevant mechanisms for polymerization; specifically step-growth and chain-growth methods.¹³ These methods provide polymers with distinctly different structures in terms of repeat unit functionality, molecular weight, and dispersity. As these molecular structures relate to higher-level macromolecular considerations, such as chain-chain interactions and the development of material morphology, it is important that the mechanism be understood for any system under study. Step-growth polymerization sees the step-wise buildup of molecular weight as a function of the extent of conversion of reactive monomer functional groups. As taught by Carother's equation, high molecular weight polymers are obtained at high extents of conversion requiring especially high degrees of monomer purity. The excess of any one monomer type (more formally the excess of any one functional group in polymerization) limits the molecular weight considerably where oligomers can provide non-optimal properties.

Chain-growth polymerizations to form addition polymers are most often accomplished using monomers with multiple bonds and loss of unsaturation. In this mechanism, a reactive intermediate is first created in an initiation step and subsequently propagates *via* repeated monomer addition to provide a macromolecule. When the reactive intermediate is ionic, impurity termination or quenching processes can kill the reactive intermediate, while in the case of radical polymerization, coupling termination can lead to an overall doubling of the average molecular weight. Many early attempts at forming conjugated polyarylenes and polyheterocycles attempted to use step-growth polymerization under non-optimized conditions, thus yielding low molecular weight polymers. Significant efforts detailed in this book demonstrate how careful control of the reagents and polymerization conditions now lead to quality polymers as high molecular weight, well-defined chemical systems. In fact, in some instances where it was believed that step-growth couplings were occurring, detailed studies show that indeed chain-growth (and in some instances living) polymerizations were in fact underway. While one of the benefits of a chain-growth polymerization can be the formation of high molecular weight polymers at a low degree of monomer conversion, the fact that unsaturation is

lost tends to limit simple chain-growth polymerizations to directly form conjugated polymers to alkyne derivatives.

1.3 Side Chains, Processability and Molecular Weight

One of the most important physical limitations that have been addressed by synthetic chemists over the years is the inherent insolubility of pi-conjugated polymer chains. With a tendency towards rigidity and strong interchain pi-stacking interactions, the inherent systems tend to be completely insoluble and infusible, as illustrated by the structures of unsubstituted ($R=H$) polythiophenes (**4**), poly(*p*-phenylenes) (**5**), and poly(*p*-phenylene vinylene) (**6**). A major success of synthetic efforts over the years has been to create highly soluble pi-conjugated polymers that can be processed into thin-film and fiber forms for potential applications. Overcoming these solubility issues was one of the most important early contributions the synthetic community made to the field. The introduction of pendant flexible side chains ($R = \text{alkyl}$ and alkoxy in **4**, **5**, and **6**) on conjugated polymers provides conformational entropy that induces solubility into the polymer product. As a generality, alkyl groups on the order of 6–8 carbons in length (hexyl to octyl), provide sufficient conformational disorder to induce solubility in the high molecular weight polymers with simple single aryl ring repeat units. This method is illustrated throughout this text, as it has become the main approach for preparing usefully processable conjugated polymers (Chart 1.2).

Considering the high molecular weights possible with chain-growth polymerizations, the synthesis of soluble and processable polymer precursors to fully conjugated materials has proven to be an excellent route for preparing useful materials. An early example of this is the synthesis of poly(*p*-phenylene vinylene) (PPV) *via* the polymerization of bis-sulfonium salts of bis-dichloromethylbenzene.^{14,15} Basic treatment of the bis-sulfonium salt leads to *in situ* formation of a quinoidal structured intermediate (not isolated), which subsequently polymerizes to form a nonconjugated polyelectrolyte that is soluble in alcoholic media. This soluble precursor polymer solution can be stored for quite some time, and subsequently processed into thin films by any number of solution processing methods. Thermal treatment of the solid material leads to elimination of HCl and dialkylsulfide or tetrahydrothiophene yielding the final conjugated PPV derivative. This general concept of soluble precursor polymer synthesis has found use in the preparation of various polyacetylenes,¹⁶ poly(*p*-phenylenes),¹⁷ and poly(thienylene vinylenes)¹⁸ along with numerous other

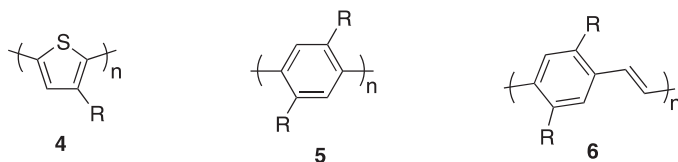


Chart 1.2

poly(arylene vinylene) systems in general. A major benefit of this methodology is that high molecular weight polymers can be obtained, even at low monomer conversion, with the precursor polymers tending to solution process well. A major drawback of the polymer precursor route is the chemical purity of the final conjugated polymer. As with any reaction on a macromolecule, complete conversion is not possible. In addition, many of the conversion reactions are thermally driven eliminations where side reactions are induced.

A standard question asked in any new polymer study is, what is the magnitude of the molecular weight that is required to provide the limiting properties for a particular application? This will be an important concept addressed throughout the many chapters in this book, as the polymerization chemistry used to attain conjugated systems can be quite varied. As just one example, consider the evolution of the optical absorption spectra of conjugated polymers as a function of chain length and the effect on the resultant color (important when considering electrochromic applications) transmitted or reflected by the final polymer films. In a combined size exclusion chromatography/UV-Vis spectroscopy experiment, it was found that a series of cyanovinylene-linked dioxithiophene polymers attained their limiting spectra at a GPC estimated number average molecular weight of approximately 10 kg/mol.¹⁹ Simultaneously, this molecular weight also provided materials with sufficient film-forming properties for stable and reproducible electrochemical switching and, as such, this molecular weight is adequate for this specific electrochromic polymer application. In general, many step-growth polymerization methodologies can provide conjugated polymers of sufficient molecular weight for the application at hand where the materials are used as thin, electrode-supported, films. Standard equilibrium controlled step-growth polymerizations have degrees of polymerizations controlled by Carother's equation. The necessity for a high degree of functional-group conversion for molecular weight creates the situation in which the synthetic chemist must be especially careful about monomer purity and functionality. At the same time, it has been demonstrated that higher molecular weights, beyond which there is no visible change in the spectroscopic signature of a conjugated polymer, can provide elevated power conversion efficiencies in solar cell and field effect transistor applications.²⁰ These considerations of molecular weight are subtle from polymer to polymer, and application to application, and must be addressed separately for each system. These concepts are illustrated nicely throughout this book.

1.4 Structural Control *via* Repeat Unit and Functionality

When one considers how synthetic chemistry has impacted the development of conjugated polymers, there is no better example than the poly(3-alkylthiophenes) (P3ATs, **4**). Early work focused on oxidative polymerization methods as a means of preparing soluble forms of this polymer.²¹ Subsequently, Grignard coupling reactions were able to prepare the polymer directly in the

reduced state, such that there were no residual charge carriers in the materials (this would ultimately prove useful in the concepts of using P3ATs as semi-conducting and charge-transporting organic electronic materials).²² Disorder through the formation of head/head and tail/tail defects led researchers to develop controlled polymerizations that provided regioregular P3ATs with a high degree of order.²³ Even finer control has been brought through the utilization of Grignard metathesis reactions and the examination of polymerization catalytic processes, such that the polymerization can be carried out under living conditions.²⁴ It is just these considerations that are the major driving force that led us to edit this book. It is crucial that synthetic chemists obtain polymers with high repeat unit purity, backbones with no branching or crosslinking, high molecular weights with low dispersity, and overall high purity in the removal of residual chemical species formed during polymerization, such as entrapment of metallic catalyst impurities. Further, the controlled introduction of end groups on the conjugated polymer chains provides another degree of purity, and depth of structural understanding.

This book is designed to provide the reader with a comprehensive view of how the various classes of conjugated polymers are synthesized. Contained within these 20 chapters are overviews of the reactions, structures, and synthetic conditions required for effective polymer formation, along with experimental details. Throughout the text, the evolution of structural build up is a focus; moving from simple polymer repeat units, to highly functionalized polymers, to more complicated structures with specific property design in mind. Building on the fundamental conjugated polymer systems introduced above, a number of chapters are directed to various forms of polyarylenes such as the poly(phenylene ethynylenes) (**7**, Chapter 8), polyfluorenes (**8**, Chapter 5), and polycarbazoles (**9** and **10**, Chapter 6), to name just a few. Property modification becomes evident through the extent of conjugation provided in these types of polymers. For example, comparison of the 2,7- and 3,6-linked polycarbazoles allow examination of the effects of full compared to broken conjugation, where the latter structure leads to discrete chromophores. Ultimately, the ability to form these specific linkages in polymers plays an important role in determining ultimate properties as the 2,7-linked carbazole units are found to be useful in high-performance solar polymers,²⁵ while the electron-rich 3,6-linked carbazoles find use in easily switchable, redox-active electrochromic polymers²⁶ (Chart 1.3).

As noted earlier, polythiophene has served as an easily functionalized system where the nature of the side chains, and their regio-orientation, provides a

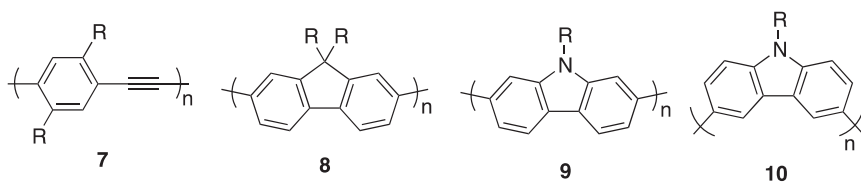


Chart 1.3

broad range of controllable solution and solid-state order properties. Many functionalized conjugated polymers are illustrated throughout this collection of chapters where the side chains bring added functionality. Using the oligoether and naphthylene containing side-group-substituted polythiophenes **11** and **12**, respectively, (Chapter 9) as examples, polar ion coordinating and liquid-crystalline behavior can be introduced into the resultant materials. Dioxythiophene chemistry, led by poly(3,4-ethylenedioxythiophene) (PEDOT) (Chapter 10),²⁷ provides a class of polymers that are easily oxidized, thus providing highly stable conducting materials. The poly(3,4-propylenedioxythiophene) (PProDOT, **13**) family of polymers can be prepared using oxidative, Grignard metathesis, and direct arylation conditions to yield a family of polymers that are especially vibrantly colored in their neutral states and transmissive in their oxidized forms, as desired for electrochromic applications²⁸ (Chart 1.4).

The range of properties introduced by side chains on conjugated polymers is quite broad and can include redox activity, charge transporting capabilities, optical absorption and emission, and chemical reactivity. This is illustrated by the two polyfluorenes, **14** and **15** (Chapter 5), which are functionalized with electron-rich and hole-transporting groups. In these polymers, light emission is provided by the polymer backbone, while the charge-carrying properties are dominated by the pendant side chains. Synthetic chemistry employed in preparing conjugated polymers with functional side chains must take their potential reactivity (such as ease of oxidation) into account, an aspect that is nicely illustrated throughout this book (Chart 1.5).

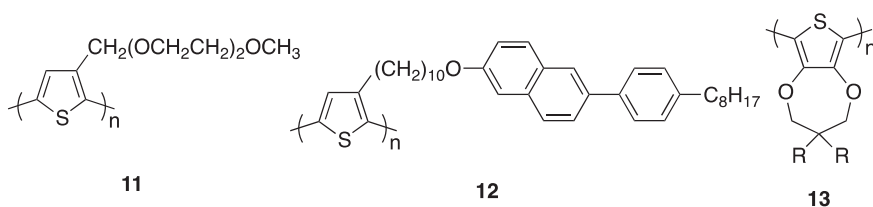


Chart 1.4

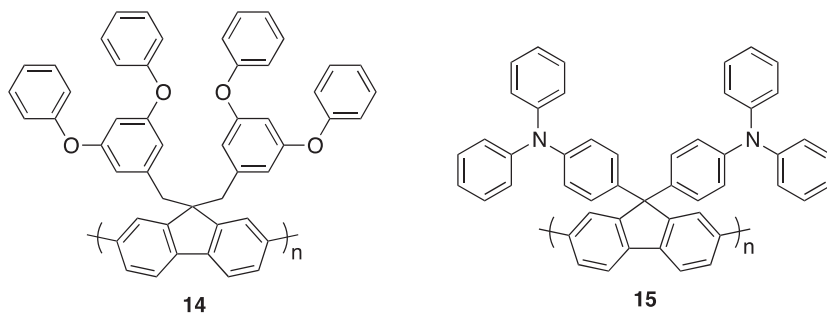


Chart 1.5

As synthetic chemists desired to tune the optoelectronic and redox properties of conjugated polymers in a fine manner, more complicated conjugated systems were required. The two fused heterocycles-substituted polythiophenes **16** and **17** (Chapter 18) illustrate this as electron-poor imine functionality in **16** brings donor–acceptor character to the material, while the more electron-rich thio-based system **17** provides for especially easy oxidation. Polymerization of these complicated bis-2-thienyl monomers by electrochemical methods paves the way for fundamental structure–property relationships to be understood, ultimately directing the synthetic chemist towards soluble polymers (Chart 1.6).

Initiated around concepts of self-doping in which an anion is covalently bound to a pi-conjugated redox-active polymer and provided charge balance during oxidative doping in **19** and **20**,^{29,30} the synthesis of ion-containing conjugated polymers has required a unique set of synthetic capabilities. While early work focused on controlling the dominant ion transport during redox switching, many derivatives, such as that shown in the poly(*p*-phenylene vinylene) (**21**) and poly(*p*-phenylene) (**22**) derivatives, led to water-soluble polymers. Due to their amphiphilic nature, a number of these ionic polymers have been processed *via* solution methods (*e.g.* layer-by-layer film formation) and are used as active materials for sensing applications, exemplified by the highly fluorescent poly(*p*-phenylene ethynylene) derivative **23**. The use of organic solvent soluble precursor polymers that could be purified prior to conversion to their ionic forms gave a synthetic route to more structurally defined and pure conjugated polyelectrolytes (Chapter 16)³¹ (Chart 1.7).

Polyheterocycle synthesis has been especially prevalent in the synthesis of new polymers for organic electronic and photovoltaic applications.^{32,33} Revolving around a series of metal-mediated coupling reactions (Heck, Suzuki, Kosugi–Migita–Stille, direct arylation, *etc.*) electron-rich donor (D) and electron-poor acceptor (A) monomer units are combined in DA polymer motifs that allow fine control over the redox and electronic states of the pi-conjugated system. Examination of structures **24** and **25** shows the subtle synthetic control chemists have used in providing new and optimal structures in polymers designed for bulk heterojunction solar cells.^{34,35} For example, the use of

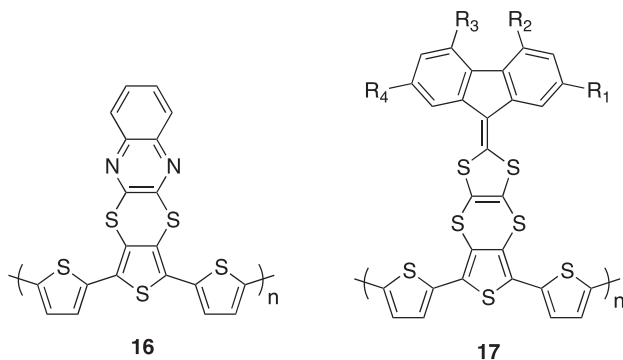
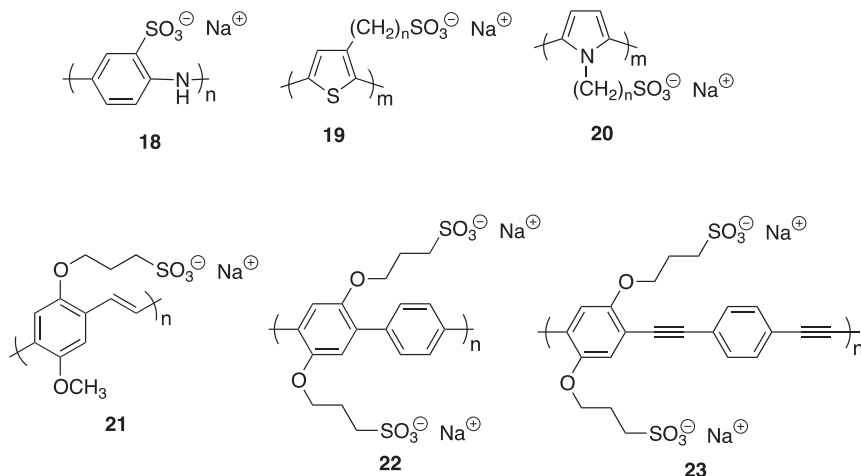
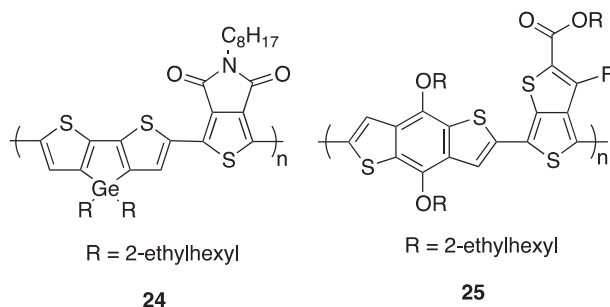


Chart 1.6

**Chart 1.7****Chart 1.8**

germanium (replacing carbon and silicon) in **24** controls bond length and stacking, while the incorporation of fluorine in **25** tunes electronic properties, such that organic solar cells constructed using both of these polymers provide high AM 1.5 power conversion efficiencies in excess of 8% (Chart 1.8).

1.5 Summary

It is evident from this collection of repeat-unit structures that synthetic chemistry, both at the molecular and macromolecular levels, is the enabling science for the preparation of a host of new materials with a broad array of properties. The collection of chapters assembled in this book address the structural and experimental details that are required for the preparation of the main classes of pi-conjugated polymers in high quality. It is hoped that both those having a general interest in the field, and those that are actively involved in the laboratory synthesizing these materials, will find this text useful and enjoyable.

Acknowledgements

Technical assistance from Mr. James Ponder during the assembly of this manuscript is greatly appreciated.

References

1. H. J. Letheby, *Chem. Soc.*, 1862, **15**, 161–163.
2. A. Dall’Olio, G. Dascola, V. Varacca and V. Bocche, *C. R. Acad. Sci.*, 1968, **433**, 267C.
3. E. T. Strom and S. C. Rasmussen, ed., “*Electrically Conducting Plastics: Revising the History of Conjugated Organic Polymers*” In *100 + Years of Plastics. Leo Baekeland and Beyond*, Strom, ACS Symposium Series #1080, American Chemical Society, Washington, DC, 2011.
4. T. A. Skotheim, ed., *Handbook of Conducting Polymers*, 1st edn, Marcel Dekker, Inc., New York, NY, 1986.
5. T. A. Skotheim, R. L. Elsenbaumer and J. R. Reynolds, ed., *Handbook of Conducting Polymers*, 2nd edn, Marcel Dekker, Inc., New York, NY, 1998.
6. T. A. Skotheim and J. R. Reynolds, ed., *Handbook of Conducting Polymers*, 3rd edn, CRC Press, Boca Raton, FL, 2007.
7. J. J. Eisch, *Organometallics*, 2012, **31**, 4917–4932.
8. H. Shirakawa, *Angew. Chem. Int. Ed.*, 2001, **40**, 2574–2580.
9. D. J. Berets and D. S. Smith, *Trans. Faraday Soc.*, 1968, **64**, 823–828.
10. T. Ito, H. Shirakawa and S. Ikeda, *J. Polym. Sci.*, 1974, **12**, 11–20.
11. C. K. Chiang, C. B. Fincher, Jr., Y. W. Park, A. J. Heeger, H. Shirakawa, E. J. Louis, S. C. Gau and A. G. MacDiarmid, *Phys. Rev. Lett.*, 1977, **39**, 1098–1101.
12. J. Ferraris, D. O. Cowan, V. Walatka Jr. and J. H. Perlstein, *J. Am. Chem. Soc.*, 1973, **95**(3), 948–949.
13. G. Odian, *Principles of Polymerization*, 4th edn, Wiley-Interscience, Hoboken, NJ 2004.
14. R. A. Wessling and R. G. Zimmerman, U.S. Patent, 3,401,152, Sept. 10, 1968.
15. D. R. Gagnon, J. D. Capistran, F. E. Karasz, R. W. Lenz and S. Antount, *Polymer*, 1987, **28**, 567–573.
16. T. M. Swager, D. A. Dougherty and R. H. Grubbs, *J. Am. Chem. Soc.*, 1988, **110**(9), 2973–2974.
17. D. G. H. Ballard, A. Courtis, I. M. Shirley and S. C. Taylor, *Chem. Commun.*, 1983, 954–955.
18. K. Jen, M. Maxfield, L. W. Shacklette and R. L. Elsenbaumer, *Chem. Commun.*, 1987, 309–311.
19. B. C. Thompson, Y. G. Kim, T. D. McCarley and J. R. Reynolds, *J. Am. Chem. Soc.*, 2006, **128**, 12714–12725.
20. R. J. Kline, M. D. McGehee, E. N. Kadnikova, J. Liu, J. M. J. Fréchet and M. F. Toney, *Macromolecules*, 2005, **38**, 3312–3319.
21. M. Sato, S. Tanaka and K. Kaeriyama, *Synth. Met.*, 1987, **18**, 229–232.

22. K. Jen, G. G. Miller and R. L. Elsenbaumer, *Chem. Commun.*, 1986, 1346–1347.
23. T. Chen, X. Wu and R. D. Rieke, *J. Am. Chem. Soc.*, 1995, **117**, 233–244.
24. M. C. Iovu, E. E. Sheina, R. R. Gil and R. D. McCullough, *Macromolecules*, 2005, **38**, 8649–8656.
25. N. Blouin and M. Leclerc, *Acc. Chem. Res.*, 2008, **41**(9), 1110–1119.
26. C. L. Gaupp and J. R. Reynolds, *Macromolecules*, 2003, **36**, 6305–6315.
27. A. Elschner, S. Kirchmeyer, W. Lövenich, U. Merker, and K. Reuter, *PEDOT: Principles and Applications of an Intrinsically Conductive Polymer*, 1st edn, CRC Press, Boca Raton, FL, 2011.
28. A. L. Dyer, E. J. Thompson and J. R. Reynolds, *Appl. Mater. Inter.*, 2011, **3**, 1787–1795.
29. A. O. Patil, Y. Ikenoue., N. Basescu, N. Colaneri, J. Chen, F. Wudl and A. J. Heeger, *Synth. Met.*, 1987, **20**, 151–159.
30. N. S. Sundaresan, S. Basak, M. Pomerantz and J. R. Reynolds, *J. Chem. Soc., Chem. Commun.*, 1987, 621–622.
31. H. Jiang, P. Taranekar, J. R. Reynolds and K. S. Schanze, *Angew. Chem.*, 2009, **48**, 4300–4316.
32. C. Nielsen and I. McCulloch, *Prog. Polym. Sci.*, 2013, Published online, 10.1016/j.progpolymsci.2013.05.003.
33. B. C. Thompson and J. M. J. Fréchet, *Angew. Chem. Int. Ed.*, 2008, **47**, 58–77.
34. C. M. Amb, S. Chen, J. Subbiah, K. R. Graham, C. E. Small, F. So and J. R. Reynolds, *J. Am. Chem. Soc.*, 2011, **133**, 10062–10065.
35. Y. Liang and L. Yu, *Acc. Chem. Res.*, 2010, **43**(9), 1227–1236.

CHAPTER 2

Polyacetylenes

KAZUO AKAGI

Kyoto University, Department of Polymer Chemistry, Katsura Campus,
Kyoto 615-8510, Japan
Email: akagi@fps.polym.kyoto-u.ac.jp

2.1 Introduction

Since the synthesis of polyacetylene (PA) thin film and the discovery of chemical doping disclosed the uncultivated field of conductive polymers,¹⁻⁴ conductive polymers have been extensively investigated and widely used in such products as electrolytic capacitors and secondary batteries.⁵⁻⁷ Today, polymers have become essential for lightweight, high-performance batteries used in notebook computers, cellular phones, and other portable equipment. Much research and development has also been conducted on polymer light-emitting diodes, organic solar cells that are anticipated for use in next-generation displays and energy sources.⁷ Conductive polymers are also being studied for their use as materials in molecular devices, called the ultimate electronic devices.⁸ Thus, although many conductive polymers have been developed for various applications, PA is still the highest conductive polymer, showing an electrical conductivity of 10^5 S/cm after iodine doping.^{9,10}

Helical PA (H-PA) is a unique conductive polymer because it has a super-hierarchical helical structure forming a spiral morphology, and it is synthesized in an asymmetric reaction field consisting of a chiral nematic liquid crystal, even though an acetylene monomer has no chiral moiety.¹¹ Despite the helical structure, the relatively high conductivity of 10^3 S/cm allowed us to anticipate that H-PA might be a prototype exhibiting novel electromagnetic properties such as a nanosize polymer solenoid. It is intriguing to elucidate H-PA from an

interdisciplinary viewpoint between polymers, liquid crystals and synthetic metals.

2.1.1 Polyacetylene (PA)

Acetylene was first polymerized by Natta and coworkers using a Ziegler–Natta catalyst, $\text{Ti}(\text{O}-n\text{-Bu})_4 - \text{AlEt}_3$.¹² The polymer obtained was a gray, infusible, and powdery material, which was not soluble in any common solvents. It was not amenable to most characterization methods and did not possess the interesting electrical properties that were anticipated. Several other catalyst systems were shown to polymerize acetylene, yielding similar products.^{13–16} Pristine PA is a typical semiconductor, but its electrical conductivity of 10^{-9} – 10^{-5} S/cm can be varied by over 14 orders of magnitude through chemical doping.^{17,18} The maximum conductivity reported to date for mechanically stretched and highly aligned PA is more than 10^5 S/cm after iodine doping,^{9,10} which is comparable to that of copper and gold.

2.1.1.1 Shirakawa-Type PA

Using the same Ziegler–Natta catalyst employed by Natta *et al.*, but with different experimental conditions, Shirakawa and coworkers succeeded in preparing free-standing polyacetylene (PA) films having metallic luster (Figure 2.1).^{19,20} The polymerization at low temperature yields *cis* PA. The *cis* content of the polymer decreases with increasing polymerization temperature. Thus, a polymer synthesized and purified carefully at -78°C contains 98% *cis* form, whereas a polymer obtained at room temperature is about 60% *cis* (40% *trans*).²¹ Since the rate of isomerization of *cis*-rich polymer in the solid state is too slow at room temperature, heat treatment at 75°C for 300 min is necessary to obtain a polymer containing the same *trans* content as the polymer synthesized at room temperature. The *trans* PA film is an intense black material with a metallic luster (Figure 2.1), whereas the *cis* PA film has a copper-like

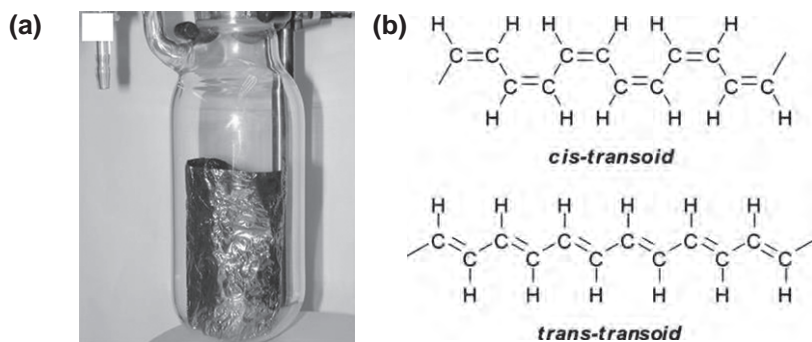


Figure 2.1 Polyacetylene film with metallic luster (a) and molecular structures (b).

luster. Very thin films of *trans* and *cis* polymers show deep blue and clear red colors, respectively.

PA has a planar structure, irrespective of *cis* and *trans* forms, due to strong π -conjugation between the sp^2 -hybridized carbon atoms in the PA polymer chain.^{22,23} Strong interchain interactions give rise to a fibrillar crystal consisting of rigid, π -stacked polymer chains.^{19,20,23} This makes PA infusible and insoluble in any kind of solvent. Thus, the solid-state structure and morphology of PA are determined during acetylene polymerization. The fibril morphology of PA films is randomly oriented, as is typical for ordinary polymers, depressing the inherent one-dimensionality of this polymer (Figure 2.2). Hence, several types of procedures and polymerization methods for macroscopic alignment of the polymer have been developed to achieve higher electrical conductivity with an anisotropic nature.^{24–34}

2.1.1.2 Mechanically Stretchable PA

PA films can be stretch-aligned to a limited degree of orientation, resulting in anisotropic electrical and optical properties.³⁵ However, it is unclear to what extent the orientation of the polymer chain contributes to these properties. Other morphological parameters are unknown, such as the distribution of crystalline and amorphous domains in the PA films, as well as their influence on physical properties of the films. Therefore, a novel synthetic method for controlling the morphology of PA during acetylene polymerization was carried out. Heeger and coworkers synthesized a partially oriented PA film by polymerizing acetylene on the surface of a biphenyl crystal.^{36,37} Despite the incompleteness of this work in obtaining macroscopically aligned PA, this experimental trial yielded an important idea for how one can control the morphology of PA *via* the polymerization of acetylene.

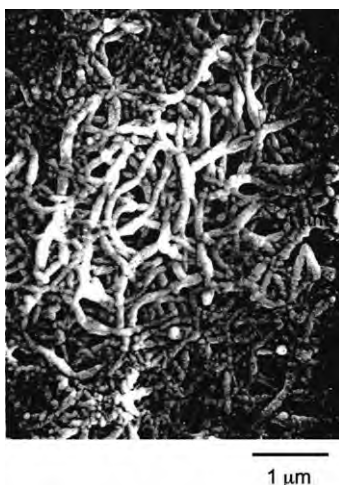


Figure 2.2 Random fibril morphology of polyacetylene film.

One approach is the mechanical stretching of an as-grown PA film.^{9,10,26–31} The conductivity of the film is enhanced through a uniaxial alignment of the fibrils associated with the mechanical stretching of the film. It is therefore desirable to develop highly stretchable PA films with high-modulus and high-tensile properties that might prevent the cleavage of fibrils and/or of PA chains during mechanical stretching. In other words, profound mechanical strengths such as Young's modulus and tensile strength are responsible for the uniaxial alignment and hence the electrical conductivity of the stretched film.

2.1.1.2.1 Naarmann and Theophilou-Type PA. Naarmann and Theophilou⁹ synthesized highly stretchable PA films using a high-temperature aged Ziegler–Natta catalyst, $\text{Ti}(\text{O}-n\text{-Bu})_4$ and AlEt_3 , dissolved in viscous silicone oil or toluene, and reported high conductivities of 10^5 S/cm after iodine doping in CCl_4 solution. Their polymerization method is characterized by use of silicone oil as a solvent, aging of the catalyst at 120°C and addition of reducing agents (ARA) such as *n*-butyllithium or Mg-derivative before polymerization.^{3,9,38} An acetylene polymerization using the aged catalyst in a silicone oil yields a homogeneous, defect-free PA film that can be stretched mechanically by up to 550%, corresponding to stretching rates of 6.5. When doped with iodine in CCl_4 , the film displays an electrical conductivity of $\sim 1.6 \times 10^4$ S/cm. An aged catalyst in a silicone oil that has been mixed with various quantities of *n*-butyllithium and allowed to react with acetylene yields PA that is highly regular, compact and crystalline in well-defined parallel planes. In special cases, the transparent films can be stretched by up to 400% ($l/l_0 = 5$) and gives a conductivity of higher than 10^5 S/cm after doping in CCl_4 . Bulk densities of the films are 0.85–0.9 and 1.12–1.15 before and after doping. The stability studies show that the *cis* fraction (70–80%), conductivity and morphology of the films are unchanged after several months. Here, it should be noted that Naarmann's method including the ARA technique lacks for reproducibility of the conductivity higher than 10^5 S/cm.³⁸ The transmission electron microscope (TEM) results indicate inhomogeneous doping within the fibrils, showing highly doped regions separated by non-doped regions, which are typically 1–3 nm wide. The temperature dependence of the dc conductivity of iodine-doped PA film can be fitted with the Sheng formula within a model of a heterogeneously conducting material consisting of highly conducting regions that are separated by insulating barriers.³⁹

2.1.1.2.2 Tsukamoto-Type PA. Tsukamoto *et al.*¹⁰ modified Naarmann's method using a higher-temperature aged catalyst dissolved in decaline and employing acetylene gas under low pressure. An SEM micrograph of unstretched PA film shows that the film is composed of a densely packed globular structure and is contrasted with the fibril structures of conventional PA. Such densely packed structure indicates a high volume density. The bulk density of PA is around 1.1 g/cm^3 . The *cis* content is estimated to be 96% and the mechanical stretchability is 8–10. The mechanically stretched films show electrical conductivities of higher than 10^5 S/cm after iodine doping.

However, all the samples do not always yield conductivity higher than 10^5 S/cm. The reproducibility is 70 to 80%.⁴⁰ As the thickness of highly conducting PA is around 1 μm , accurate thickness measurement is one of the most crucial points in determination of conductivity. Temperature dependences of conductivities of fully iodine-doped PA were measured in the temperature range between 12 K and 300 K. The temperature dependence shows that activation-type conduction is still dominant in this temperature range, just as does that of doped conventional PA. Namely, the temperature dependence of conductivity is not metallic, suggesting that interdomain and interfibrillar processes are still dominant in the conductivity.

2.1.1.2.3 High Mechanical Modulus and Strength PA. Akagi *et al.*^{24,25} developed two solvent-free acetylene polymerization methods: a solvent-evacuation (SE) method and an intrinsic nonsolvent (INS) one. In the former, cumene used as a solvent is evacuated after the high-temperature aging of the catalyst. In the latter, no solvent is used from the preparation and high-temperature aging of the catalyst to the polymerization. PA films synthesized by these methods exhibit extremely high mechanical strengths characterized by a Young's modulus of 40–100 GPa and a tensile strength of 0.9–2.1 GPa,^{24,41} comparable to those (132 and 3.9 GPa) of well-known engineering plastics such as Kevlar, in addition to a high bulk density of more than 1.0 g/cm^3 . The films show well-reproducible and high conductivities of $2.2\text{--}4.3 \times 10^4$ S/cm, which are enhanced by the uniaxial alignment of polymer chains associated with a mechanical stretching of 8–9 times. It can be noted from these results that the high mechanical strength is a prerequisite for the achievement of high electrical conductivity, and that in the INS polymerization, the cocatalyst of AlR_3 , by virtue of its liquidity, plays the role of a solvent toward catalytically active complexes formed between $\text{Ti}(\text{OR})_4$ and AlR_3 , which guarantees the homogeneity of the catalyst system in spite of the absence of solvent.⁴²

The ESR studies^{43,44} show that high-temperature aging at 150–200 °C on the $\text{Ti}(\text{O}-n\text{-Bu})_4$ and AlEt_3 catalyst yields a bulky aggregate of Ti^{3+} complex with a bridged structure through butoxy and/or ethyl groups. Such a bulky complex should lead to a decrease of apparent catalytic activity and hence a depression of the exothermic heat associated with the acetylene polymerization. This allows a moderate condition that guarantees production of a *cis*-rich and highly homogeneous PA film.

The numerical evaluations based on the analytical formulae⁴⁵ indicates that the inplane alignment contributes to enhance the conductivity of the aligned film in a cooperative manner with the mechanically forced fibril alignment (parallel alignment). In particular, the inplane alignment becomes crucially dominant when the film thickness is less than 1.0 μm . On the other hand, although the parallel alignment expectedly decreases the conductivity perpendicular to the elongation direction along with the mechanical stretching, the decrease is partly compensated by an increase due to the inplane alignment.

2.1.1.3 Directly Aligned PA

Another approach is a direct alignment of the film using a liquid crystal as an anisotropic solvent for acetylene polymerization under an external perturbation such as gravity flow and magnetic field.^{32–34} This approach affords an alignment of even ultrathin films with semitransparency that is suitable for measurements of nonlinear optics.⁴⁶ A nematic LC (N-LC) has long-range orientational order. Furthermore, the orientational order of a N-LC can be easily controllable using external perturbations, such as an electric field, magnetic field, sheer force, or gravity flow. For this reason, N-LC is useful for an anisotropic reaction solvent for controlling the morphology of PA during acetylene polymerization. N-LCs that could be used as solvents for the Ziegler–Natta catalyst are limited, because they can act as reactive substituents with the active species and/or components of the catalyst. Among the available N-LCs, a phenylcyclohexane (PCH) derivative is stable in the presence of Ziegler–Natta catalyst.^{32–34}

Acetylene polymerization was carried out under a gravity flow of the LC reaction field, in which the Ziegler–Natta catalyst was dissolved. Macroscopically aligned fibrils were found along the gravity flow direction of the N-LC catalyst solution. The direction of fibril growth appeared to coincide with that of N-LC molecules under the gravity flow of the solution. In fact, PA chains propagate along the director (average direction of LC molecules within a domain) of the N-LC. This novel and simple method produces highly oriented PA films, making it possible to investigate various anisotropic properties of PA.^{32–34,47}

An N-LC molecule can be aligned using an external magnetic field by virtue of its anisotropy in diamagnetic susceptibility. In particular, LC molecules with positive or negative anisotropies in diamagnetic susceptibility were aligned parallel or perpendicular to the magnetic field direction, respectively. Akagi *et al.*³⁴ constructed a monodomain structured LC reaction field from a multidomain one, using an external magnetic field 2–14 kG. Owing to the positive anisotropy in diamagnetic susceptibility of the phenyl moiety in the LCs, the multidomain structure of N-LCs tends to be aligned in parallel with the magnetic field direction, making a monodomain structured N-LC. Highly aligned PA was synthesized in a monodomain structured LC reaction field (Figure 2.3).^{34,48,49}

The macroscopically aligned PA films prepared in N-LCs under magnetic field show high conductivities of 10^4 S/cm after iodine doping, and anisotropies of ca. 5 defined as a ratio of parallel to perpendicular to the aligned fibril direction. The unexpectedly small anisotropy is attributed to the relatively high conductivity in the perpendicular direction. This is because the aligned film has highly condensed fibril morphology and hence the interchain and even interfibril hopping of the charged carrier are largely enhanced. The degree of alignment of the film is governed by that of the liquid crystal used as the solvent. That is, the morphology and therefore the macroscopic properties of the film are crucially dependent on the anisotropic polymerization field.^{48,49}

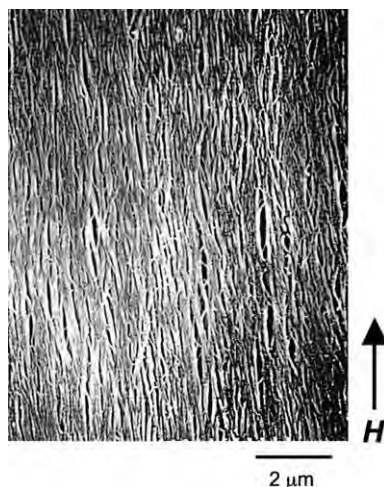


Figure 2.3 Macroscopically aligned polyacetylene film synthesized in nematic LC (N-LC) reaction field under magnetic field.

This situation is common to an epitaxial polymerization, where acetylene polymerization is carried out on the substrate crystal with a homologous isomorphous compound such as naphthalene, anthracene, biphenyl, or terphenyl.⁵⁰ The fibril orientation is strongly dependent on the lattice matching between PA and the substrate crystals.

It is worth noting here that a PA bearing an LC moiety in the side group was reported in 1993.^{51,52} The LC-substituted PA is not only soluble in organic solvents, but also easily aligned by spontaneous orientation of the LC group. In addition, it was macroscopically aligned by an external perturbation, such as shear stress, electric field, and magnetic field.^{51–56} This situation means that a monodomain structure of the LC phase can be constructed on a macroscopic level. Thus, the polymer should have a higher electrical conductivity, compared with the case of random orientation. At the same time, one can control the molecular orientation and, hence, the electrical conductivity of the polymers with an external force. As the macroscopic alignment was first achieved under magnetic field,⁵⁶ it is straightforward to study many kinds of LC-substituted PA derivatives.^{54,56–63} However, the electrical conductivity of LC-substituted PA is significantly lower than that of nonsubstituted PA. This is due to a lower coplanarity of the main chain, which arises from steric repulsion between substituents, a higher ionization potential, and a lower electron affinity.

2.1.2 Helical Polyacetylene (H-PA)

It has been generally accepted that PA has a planar structure, irrespective of *cis* and *trans* forms. This is due to π -conjugation between the sp^2 -hybridized carbon atoms in the polymer chain.^{1,19–22} If it were possible to modify this planar structure of PA into a helical one, novel magnetic and optical properties might

be expected.^{64,65} Here, we present the polymerization of acetylene in an asymmetric reaction field, which is constructed with chiral nematic LCs (N*-LCs), and show that PA films formed from helical chains and fibrils can be synthesized.^{11,66–80}

2.1.2.1 Asymmetric Liquid Crystal Reaction Field

The N*-LC to be used as an asymmetric solvent is prepared by adding a small amount of chiral compound, as a chiral dopant, into nematic LC (Figure 2.4). The formation of N*-LC is recognized when a Schlieren texture characteristic of nematic LC changes into a striated Schlieren or a fingerprint texture in a polarized optical microscope (POM). The distance between the striae corresponds to a half-helical pitch of the N*-LC. Note that as the degree of twist in the N*-LC is larger, the helical pitch observed in POM is shorter.

The helical pitch of the N*-LC can be adjusted by two methods: changing the concentration or changing the twisting power of the chiral dopant. However, the mesophase temperature region of the N*-LC is affected by changing the concentration of the chiral dopant. Namely, it becomes narrow as the concentration increases, and finally the mesophase is destroyed when the concentration is close to a critical value. Herein, owing to the limitation of the concentration method, an alternative approach of utilizing the chiral compound with large twisting power is adopted. Axially chiral binaphthyl derivatives are used as chiral dopants,⁷⁴ since they have been reported to possess larger twisting powers (HTPs) than asymmetric carbon-containing chiral compounds.⁶⁷

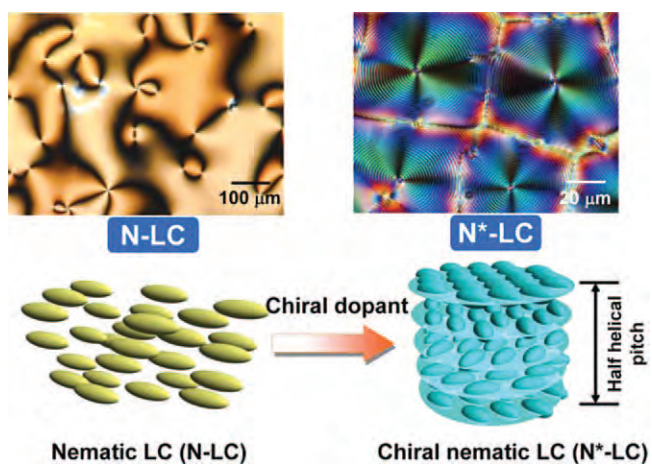


Figure 2.4 Chiral nematic liquid crystal (N*-LC) induced by the addition of a chiral dopant into N-LC. Schlieren texture (left) and fingerprint texture (right) are observed for N-LC and N*-LCs, respectively, with a polarized optical microscope.

The axially chiral binaphthyl derivatives, (*R*)- and (*S*)-1,1-binaphthyl-2,2-di-*p*-(*trans*-4-*n*-pentylcyclohexyl) phenoxy-1-hexyl]ether, are synthesized using Williamson etherification reactions of chiroptical (*R*)- and (*S*)-1,1-bi-2-naphthols, respectively, with phenylcyclohexyl derivatives. The products are abbreviated as (*R*)- and (*S*)-D-1 (Figure 2.5). To prepare an induced N*-LC, approximately 5 to 14 wt% of (*R*)- or (*S*)-D-1 is added as a chiral dopant to an equimolar mixture of the N-LCs 4-(*trans*-4-*n*-propylcyclohexyl)ethoxybenzene (PCH302) and 4-(*trans*-4-*n*-propylcyclohexyl)butoxybenzene (PCH304). The LC substituent group in (*R*)- and (*S*)-D-1 enhances miscibility between the N-LC mixture and the binaphthyl derivative used as the chiral dopant. Note that usage of similar substituents with a shorter methylene spacer such as PCH503 or normal alkyl substituent gave insufficient miscibility, yielding no chiral nematic phase. In polarizing optical micrographs of the mixture of PCH302, PCH304, and (*R*)-PCH506-binaphthyl and that of PCH302, PCH304, and (*S*)-PCH506-binaphthyl, a striated Schlieren or finger printed texture characteristic of N*-LC phase is observed.

Although each component (PCH302 or PCH304) shows a LC phase, the LC temperature region is very narrow, being less than 1 to 2 °C. This is not suitable for acetylene polymerization in a N-LC or N*-LC reaction field, because the exothermal heat evolved during the acetylene polymerization would raise the temperature inside a Schlenk flask. This would easily destroy the LC phase, making it isotropic. Hence, the LC mixture is prepared by mixing two equimolar LC components. In the LC mixture, the nematic – isotropic temperature, $T_N - I$, and the crystalline – nematic temperature, $T_C - N$, are raised and



Figure 2.5 Construction of asymmetric reaction field for acetylene polymerization by dissolving Ziegler–Natta catalyst, $\text{Ti}(\text{O-}n\text{-Bu})_4\text{-AlEt}_3$, into the N*-LC. The N*-LC includes an axially chiral binaphthyl derivatives, D-1 or D-2.

lowered, respectively. In fact, the mixture exhibits the LC phase in the region from 20 to 35 °C. Subsequently, the change of T_{N-I} upon addition of $Ti(O-n-Bu)_4 - AlEt_3$ catalyst is examined using differential scanning calorimetry (DSC). Taking into account the effect of supercooling for LCs, a catalyst solution that consists of a LC mixture and chiral dopant is obtained for room-temperature polymerization ranging from 5 to 25 °C. Note that supercooling is the process of lowering the temperature of a liquid or a LC below its freezing point without it becoming a solid. This sufficiently wide temperature region enables the performance of acetylene polymerization in the N^* -LC phase. A Ziegler – Natta catalyst, consisting of $Ti(O-n-Bu)_4$ and $AlEt_3$, is prepared using (*R*)- or (*S*)- N^* -LC as a solvent (see, Figure 2.5). The concentration of $Ti(O-n-Bu)_4$ is from 15 to 50 mM, and the mole ratio of the cocatalyst to catalyst, $[AlEt_3] / [Ti(O-n-Bu)_4]$, is 4.0. The catalyst solution is aged for 0.5 h at room temperature. During the aging, the N^* -LC containing the catalyst shows no noticeable change in optical texture and only a slight lowering of the transition temperature by 2 to 5 °C. The transition temperature between the solid and N^* -LC phases is 16 to 17 °C. The transition temperature between the N^* -LC and isotropic phases is 30 to 31 °C. No solidification is observed down to -7 °C, as a result of supercooling. Thus, the (*R*)- and (*S*)- N^* -LCs are confirmed to be chemically stable in the presence of the catalyst. It is therefore possible to employ these LCs as an asymmetric solvent for acetylene polymerization.

2.1.2.2 Characterization of H-PA

SEM images of H-PA films show that multidomains of spiral morphology are formed (Figure 2.6a), and each domain is composed of a helical structure of a bundle of fibrils with a one-handed screwed direction (Figure 2.6b). The multidomain-type fibril morphology of H-PA seems to replicate that of the N^* -LC during the interfacial acetylene polymerization. A closer observation of

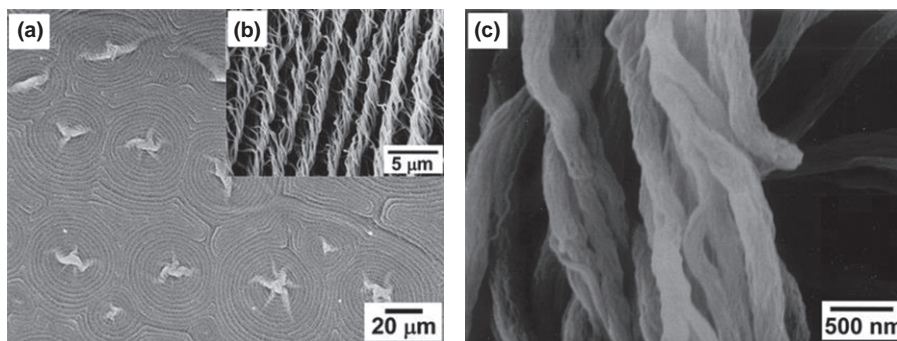


Figure 2.6 SEM micrographs of helical polyacetylene (H-PA) film synthesized in the right-handed (*R*)-System-1 {PCH302:PCH304:(*R*)-D-1 = 100:100:2 (mole ratio)} with a helical pitch of 5 μm. The photograph of (b) shows the magnified one of (a).

SEM images indicate that H-PAs synthesized in the (*R*)- and (*S*)-N*-LCs form the screwed bundles of fibrils and even screwed fibrils with left-handed and right-handed directions, respectively. This result implies that the screw direction of H-PA is controllable by choosing the helicity, *i.e.* optical configuration of the chiral dopant, so far as the N*-LC induced by the chiral dopant is employed as an asymmetric polymerization solvent. In addition, it is of keen interest that the screw directions of bundle and fibrils are opposite to those of the (*R*)- and (*S*)-N*-LCs used as solvents.

It has been elucidated so far that the PA chains propagate along the director (an averaged direction for the LC molecules within a domain) of the N*-LC. Since the helical axis of PA is parallel to the PA chain, and the director of the N*-LC is perpendicular to the helical axis of N*-LC, the helical axis of PA is perpendicular to that of N*-LC. Taking these aspects into account, one can describe a plausible mechanism for interfacial acetylene polymerization in the N*-LC, as shown in Figure 2.7. In the case of a right-handed N*-LC, for instance, the PA chain would propagate with a left-handed manner, starting from the catalytic species, but not with a right-handed one. This is because the PA chains with the opposite screw direction to that of the N*-LC could propagate along the LC molecules, but those with the same direction as that of the N*-LC would encounter LC molecules, making the propagation stereospecifically impossible. The detailed mechanism of acetylene polymerization in N*-LC has been elucidated.^{77,78}

In circular dichroism (CD) spectra of the PA thin films synthesized with (*R*)- and (*S*)-N*-LCs, positive and negative Cotton effects are observed, respectively, in the region from 450 to 800 nm. This corresponds to a $\pi \rightarrow \pi^*$ transition in the PA chain, despite the absence of a chiroptical substituent in the side chains. This indicates that the PA chain itself is helically screwed.⁶⁹ It is evident that this Cotton effect is not due to the chiral dopant, because the Cotton effect of the chiral dopant is only observed at shorter wavelengths (*i.e.* 240 to 340 nm). Left-handed (counterclockwise) and right-handed (clockwise) H-PA chains are

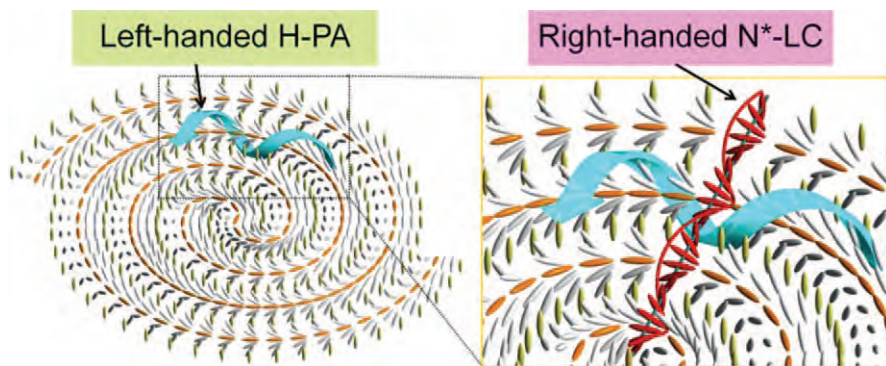


Figure 2.7 Schematic representation of mechanism for acetylene polymerization in the N*-LC. The H-PA with left-handed screw direction grows starting from the catalytic species in the right-handed N*-LC.

formed in (*R*)- and (*S*)-N*-LCs, respectively. These helical chains are bundled through van der Waals interactions to form helical fibrils.⁶⁶ The bundles of fibrils form a spiral morphology with various sizes of domains. From the results mentioned above, it is worth noting that, by using the N*-LC as an asymmetric polymerization solvent, a hierarchical helical structure having primary to higher orders in H-PA is synthesized (Figure 2.8).⁶⁶

The dihedral angle between neighboring unit cells, ($-\text{CH}=\text{CH}-$), of the H-PA is estimated to be from 0.02° to 0.23° .¹¹ Although such a very small dihedral angle may allow us to regard the present PA as an approximately planar structure, the polymer is rigorously screwed by a one-handed direction with the nonzero dihedral angle. The present H-PA films have high *trans* contents of 90% and become highly conductive upon iodine doping. In fact, the electrical conductivities of the doped films are $1.5 - 1.8 \times 10^3 \text{ S/cm}$ at room temperature, which are comparable to those of metals. The iodine-doped H-PA showed the same Cotton effect as that of nondoped PA. This indicates that the helical structure is preserved even after iodine doping. Furthermore, CD and X-ray diffraction measurements show that the helical structure is also preserved after heating to 150°C (which corresponds to the isomerization temperature from *cis* to *trans* form). The most stable structure of PA is the planar one. However, since the PA is actually insoluble and infusible, the helical structure

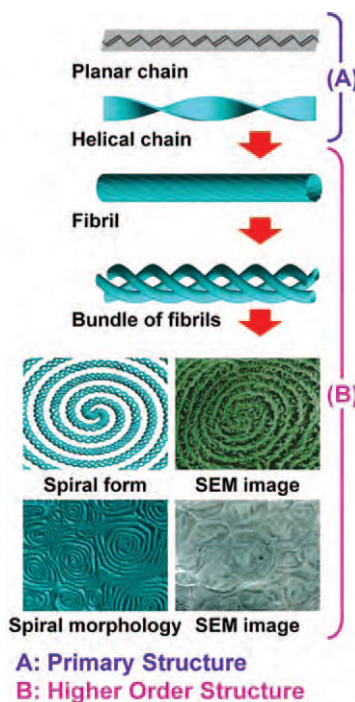


Figure 2.8 Hierarchical helical structures from primary to higher order in helical polyacetylene. SEM = scanning electron microscope.

formed during the polymerization can be preserved even if it is washed by toluene or thermally heated below the isomerization temperature. In other words, the insolubility and infusibility of PA are indispensable for preserving the metastable helical structure.

2.1.3 H-PA with Bundle-Free Fibril Morphology

H-PA is anticipated to act as a prototype of a molecular solenoid, by virtue of its helical structure and high electrical conductivity.^{64,65} It is therefore desirable to synthesize a sufficiently screwed H-PA and prevent the individual fibrils from forming bundle morphology. Toward this aim, it is essential to construct a more highly twisted LC reaction field. Here we show that a H-PA film, consisting of only single fibrils and not a fibril bundle, can be synthesized using a highly twisted N*-LC reaction field.

2.1.3.1 Powerful Helicity Inducers

It is known that binaphthyl derivatives substituted with LC groups at the 2,2',6,6' positions of binaphthyl rings exhibit good miscibility towards the host N-LC, due to their liquid crystallinities.⁶⁹ They also have HTPs based on axial chirality. However, despite using binaphthyl derivatives with large HTPs, it is difficult to induce the N*-LCs with nano-ordered helical pitches. Thus, both miscibility and large HTP are required for the effective transfer of axial chirality from binaphthyl derivatives to the host N-LCs. To investigate the amplification of HTPs in the axially chiral binaphthyl derivatives, several rigid substituent groups are introduced into the 2,2',6,6' positions of the binaphthyl rings.⁷⁴ Among them, a *tetra*-substituted binaphthyl derivative, D-2, which has a direct linkage between the mesogenic core of phenylcyclohexyl (PCH) moieties and the 6,6' position of the binaphthyl rings, shows an extremely large HTP of $449 \mu\text{m}^{-1}$ when added as a chiral dopant into N-LC (Figure 2.5, see also Scheme 2.2). The HTPs of D-1 and D-2 are $171 \mu\text{m}^{-1}$ and $449 \mu\text{m}^{-1}$, respectively. It is clear that the HTP of the chiral dopant D-2 is *ca.* 2.6 times larger than that of D-1. This may be rationalized with a difference in the number of substituents. Namely, the axially twisting torque of D-2 is more effectively transferred to environmental N-LC molecules, by virtue of intermolecular interactions between the four PCH substituents of D-2 and the PCH moieties of LC molecules. In contrast, D-1 bears only two PCH substituents.

2.1.3.2 Highly Twisted N*-LC Reaction Field

The N*-LCs, including D-1 at 1 mol% {PCH302:PCH304:D-1 = 100 : 100 : 2 (mole ratio)} and D-2 at 1.5 mol% {PCH302:PCH304:D-2 = 100 : 100 : 3 (mole ratio)}, abbreviated as System-1 and System-2, respectively, are prepared as the asymmetric reaction field for acetylene polymerization. The helical pitches of System-1 and System-2 are 5 μm and 270 nm, respectively. Figure 2.9 shows POMs of the N*-LCs, System-1 and System-2. System-1 gives a fingerprint

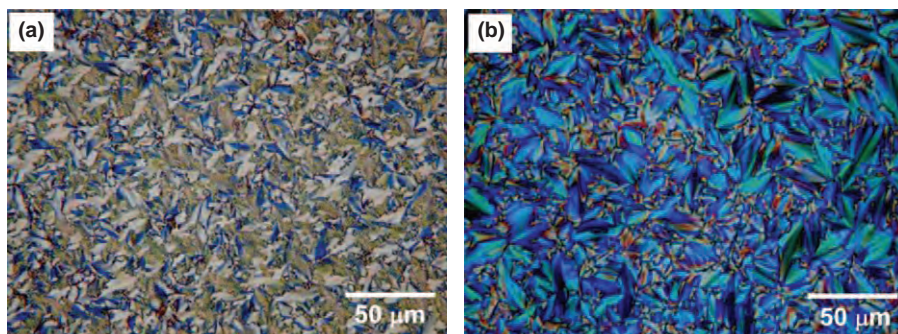


Figure 2.9 Polarizing optical micrographs of N^* -LCs at 27 °C. (a) (*S*)-System-1 containing 1.0 mol% of chiral dopant, (*S*)-D-1. (b) (*R*)-System-2 containing 1.5 mol% of chiral dopant, (*R*)-D-2.

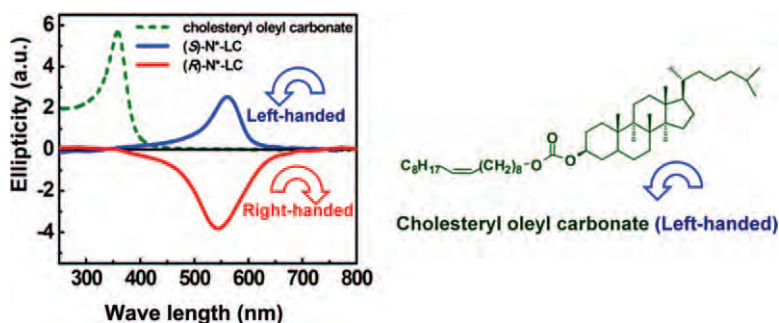


Figure 2.10 Reflection CD spectra of the cholesteryl oleyl carbonate and the N^* -LCs induced by (*R*)-D-2 and (*S*)-D-2. (*R*)- N^* -LC; PCH302: PCH304: (*R*)-D-2 = 100: 100: 2 (mole ratio). (*S*)- N^* -LC; PCH302: PCH304: (*S*)-D-2 = 100: 100: 2 (mole ratio).

texture with striae (Figure 2.9a). The distance between the striae (2.5 μm) corresponds to one half of the helical pitch in N^* -LC. Meanwhile, the POM of System-2 gives a fan-shaped texture, but no striae is observed (Figure 2.9b). This is due to the fact that the distance between the striae formed in System-2 is too small to be detected in the POM microscope, which has a resolution limit of *ca.* 1 μm .

The helical sense of System-2 is examined through a selective light reflection in circular dichroism (CD) spectra.⁶⁶ It is known that cholesteryl oleyl carbonate is a left-handed cholesteric LC that shows a selective light reflection in the visible region. Therefore, cholesteryl oleyl carbonate is used as a reference for determining the handedness of the N^* -LC. As shown in Figure 2.10, the N^* -LC inducing (*R*)-D-2 shows a negative sign, while the N^* -LC including (*S*)-D-2 and cholesteryl oleyl carbonate shows peaks having a positive sign in the CD spectra. These results indicate that the helical senses of the (*R*)- and (*S*)- N^* -LCs are right and left directions, respectively.

2.1.3.3 Synthesis of H-PA with Bundle-Free Fibril Morphology

Figure 2.11 show scanning electron microscope (SEM) photographs of the H-PA films synthesized in a right-handed N*-LC with a helical pitch of 270 nm {(S)-System-2}. Hierarchical helical structures are observed in H-PA film. It is confirmed that the screw direction of the fibril, including even the fibril bundle, is opposite to the helical sense of the N*-LC. For instance, in the right-handed N*-LC of (R)-System-1, the fibrils are screwed left to form the fibril bundle. Similarly, in the left-handed N*-LC of (S)-System-2, the fibrils are screwed right, although no bundle is formed.⁶⁹ It is of particular note that the highly twisted N*-LC (System-2) gives the fibrils but not the fibril bundle (Figure 2.11). This is in distinct contrast to the morphology of H-PA that is synthesized in the moderately twisted N*-LC (System-1). It is evident from Figures 2.11b and c that the PA fibrils synthesized in (S)-System-2 are more highly twisted than those in (R)-System-1 (see also Figure 2.6).

To elucidate the relationship between the helical pitch degree of the N*-LC and the morphology of H-PA, various N*-LCs are prepared with helical pitches between 5 μm and 270 nm (*i.e.* 2.3 μm , 850 nm, and 470 nm), by changing the mole percent of the D-2 chiral dopant. The N*-LC with a helical pitch of 2.3 μm gives the fibril bundle in H-PA morphology. In the case of the N*-LC with a helical pitch of 850 nm, bundles consisting of several fibrils are observed. The distance between bundles is less than 550 nm. When the N*-LC having a helical pitch of 470 nm is used, almost only single fibrils are observed; however, portions of the fibrils are overlapped. These results indicate that the morphology of H-PA is dominated by the helical pitch degree of the N*-LC, but not by the species of the chiral dopant.

Figure 2.12 shows a schematic representation of the relationship between the twisting degree of the N*-LC and the hierarchical morphology of H-PA. In the weakly twisted N*-LC, PA fibrils (diameters from 70 to 120 nm) are gathered to form fibril bundles (diameters up to 1 μm). Interestingly, the distance between

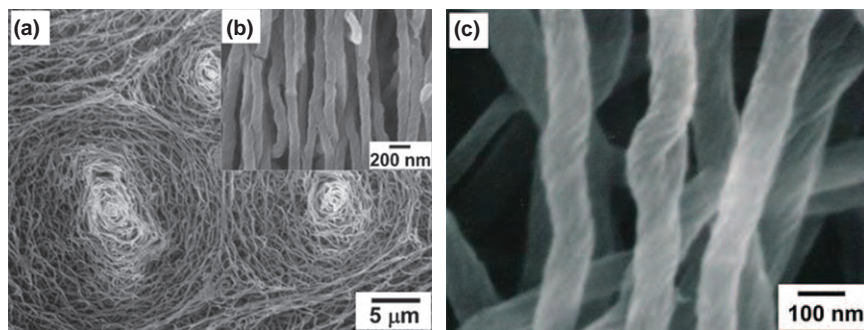


Figure 2.11 SEM micrographs of helical polyacetylene film synthesized in the left-handed (S)-System-2 {PCH302 : PCH304 : (S)-D-2 = 100 : 100 : 3 (mole ratio)} with a helical pitch of 270 nm. The photograph of (b) shows the magnified one of (a).

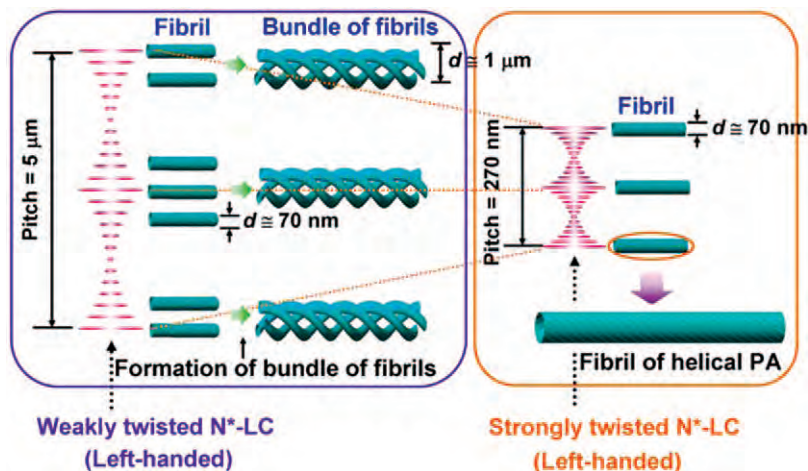


Figure 2.12 Relationship between the twisting degree of N*-LC and the morphology of helical polyacetylene.

fibril bundles is close to one half of the helical pitch. Fibril bundles can be formed in N*-LCs with helical pitches up to 1 μm . However, in the highly twisted N*-LC (helical pitch narrower than 1 μm), the PA has highly screwed fibrils, but not a bundle of fibrils. Therein, the diameters of the fibrils are in the range from 70 to 120 nm. This may be due to the fact that the helical pitch of 270 nm in the strongly twisted N*-LC is smaller than the diameter (*ca.* 1 μm) of the fibril bundle. This situation might prevent the formation of fibril bundles. This type of morphology that is free from fibril bundles should make it much easier to evaluate the electromagnetic properties of the screwed fibril.

H-PA films having a morphology free from fibril bundles have high *trans* contents of 90%. This is mainly due to the polymerization temperature of 20–21 $^{\circ}\text{C}$. It is known that the *cis* form of the PA segment is a kinetically favorable product, because of the so-called *cis* opening mechanism of acetylene polymerization. On the other hand, the *trans* form is a thermodynamically stable product. The *cis* form is actually transformed into the *trans* form, depending on the degree of exothermal heat produced during acetylene polymerization. As exothermal heat is evolved in the polymerization at 20 $^{\circ}\text{C}$, the *cis*–*trans* isomerization is enhanced to give high *trans* content in the present H-PA.⁷⁶ H-PA shows high electrical conductivities, such as around 1.8×10^3 to 2.0×10^3 S/cm, at room temperature after iodine doping. Meanwhile, the PA films synthesized in Systems-1 and 2 have bulk densities of *ca.* 0.5 and 0.96 g/cm², respectively. This indicates that single fibrils give a more closed morphological packing than the fibril bundle structure.

By virtue of the high helical twisting power and liquid crystallinity of the novel *tetra*-substituted binaphthyl derivative (D-2), we obtain a N*-LC with a helical pitch in the nanoregime. This is performed by adding a high mole percentage of chiral dopant to the N-LC without destroying the LC phase.

The helical pitches (270 to 850 nm) are smaller than the radius (1 μm) of the fibril bundle of H-PA. In particular, the highly screwed N*-LC (helical pitch of 270 nm) depresses the formation of the fibril bundle, resulting in a bundle-free fibril morphology consisting of single fibrils. Thus, we find that the degree of screwing in the N*-LC reaction field is a key factor in controlling the bundle formation and/or depression in PA fibril morphology. It is expected that a highly twisted H-PA without the fibril bundle might be feasible for the evaluation of unprecedented electromagnetic properties of a single fibril of conducting polymer. It is worth emphasizing that by using the N*-LC as an asymmetric polymerization solvent, helix formation is possible not only for PA but also for aromatic π -conjugated polymers without chiral substituents on the side chains.^{66,79,80}

2.1.4 Morphology-Retaining Carbonization of H-PA

Lastly, it is of particular interest that the H-PA film is useful as a precursor for helical carbon and graphite film when the morphology-retaining carbonization *via* an iodine doping is used.^{81,82}

It has been considered difficult to prepare a freestanding carbon thin film through the carbonization of an organic polymer film. This is because carbonization at high temperatures causes thermal decomposition and volatilization of hydrocarbon gases, destroying the morphology of the original film. However, the iodine-doped PA film was almost completely carbonized at temperatures above 800 °C. No indication of thermal decomposition was observed in differential thermal analysis curve for the doped PA film. Surprisingly, the fibrous morphology of the original structure remained unchanged, even after carbonization and heat treatment. In addition, the weight loss of the films due to carbonization at 800 °C was very small, amounting to only 20% of the film weight before iodine doping. Thus, the nanofibril-fabricated carbon film was obtained through carbonization of the doped PA film. It is elucidated that iodine doping prevents the PA film from thermally decomposing at high temperatures. According to the structural model of the iodine-doped PA film, polyiodide ions (*e.g.*, I_3^- and I_5^-) are situated between the PA chains, forming a charge-transfer complex. Iodine tends to react with hydrogen at high temperatures. Actually, outgassing of hydrogen iodide was detected by gas chromatography mass spectrometry during heating of the doped PA film. It can be assumed that hydrogen contained in the doped PA is removed to some extent as hydrogen iodide from the PA chains, and that the PA chains partially crosslink between the neighboring chains. Furthermore, most of the hydrogens are removed with increasing temperature. As a result, networks of sp^2 hexagonal carbon bonds are formed during carbonization. It should be emphasized that the carbon film heat treated at 2600 °C had almost the same helical structure as those of the original H-PA film and the carbon film that was prepared at 800 °C. We found a new aspect of the iodine doping by disclosing its indispensable role in maintaining the nanostructure and morphology of precursors during carbonization.